# Investigation into Geometric Parameters of an Inverted Airfoil in Ground Effect with the Utilization of Classic Optimization Techniques

Undergraduate Research Thesis

Presented in Partial Fulfillment of the Requirements for the Degree of Bachelor of Science with Research Distinction at The Ohio State University

By

Matthew Aultman

The Ohio State University

2017

Professor Clifford A. Whitfield, Advisor

Professor Richard Freuler

Jacob Allenstein

Department of Mechanical and Aerospace Engineering

January 2017

## Abstract

In competitive automotive racing, wing aerodynamics have been utilized since the 1960s to reduce lap time. Studies show that the near ground proximity of the race car's front wing aerodynamically enhances the wing's performance. Despite these studies, little is publicly released on the design of wings for the ground proximities experienced in automotive racing. For this study, the modified NACA 4 Series airfoil family was selected to investigate the impact that airfoil geometry has on the aerodynamic characteristics of an inverted wing in ground effect. Due to the large number of airfoil geometries required to test, ANSYS Fluent, a CFD software, was utilized to predict aerodynamic effects. Trend lines were developed for fundamental geometric shape changes of an inverted NACA 6612-63 at five degrees angle of attack and a height of fifteen percent chord from the lowest point of the airfoil. These trends were then utilized in determining which geometric parameters would be selected to study the effects of coupling using graphical optimization techniques. The trends would be further implemented in defining performance constraints in the optimization process.

**Acknowledgements**

First and foremost, I would like to thank my advisor, Dr. Cliff Whitfield, for all of his guidance and wisdom throughout the entire research process. Cliff, I cannot thank you enough for taking the time to "reign in my enthusiasm" and ensure I was always pointed in the right direction. The experience and knowledge I have gained throughout this process has been immeasurable in its importance to me.

I would like to thank my parents for all of their love and support throughout the entirety of my life. I would especially like to thank them for their support throughout my college career to ensure I did not have to work to death to maintain my finances which allowed for me to work to death on other projects such as this. Dad, you always told me if I got a job in a field I enjoyed I would never work a day in my life. Well, I enjoyed every second of this. Mom, you were always worried that I was running myself into the ground. Unfortunately, all I can say is I have not even begun to run myself into the ground yet. I hope you guys are proud.

I cannot thank my fiancé, Gabby, enough for all of her love and support over the years. Honey, I am so glad that you have been tolerant and accepting of all of the late nights throughout my research and years of school. I could not have gotten through it without you.

Finally, I would like to thank Dr. Richard Freuler and Jacob Allenstein for being on my committee. Their advice and expertise has been greatly appreciated and something I will keep with me for the rest of my career.

## Table of Contents

**Abstract……i**

**Acknowledgements……ii**

**List of Figures……v**

**List of Tables……...…….vii**

**Chapter 1: Introduction……1**

1.1: Introduction……...1

**Chapter 2: Methodology……6**

2.1: ANSYS Fluent……..6

2.1.1: Turbulence Models……6

2.1.2: Mesh……...7

2.1.3: Final Model……9

2.2.1: Set-Up……..……13

2.2.2: Procedure (Single Variable Geometry)……...…….13

2.2.3: Generation of Airfoil Coordinates (JAVAFOIL)……15

2.3: Single Variable Trends……...16

2.4: Optimization……...16

**Chapter 3: Results and Discussion……17**

3.1: Single Variable Trends……...17

3.2: Trends for Varying Maximum Camber……..22

3.3: Trends for Varying Maximum Camber Location……...26

3.4: Trends for Varying Maximum Thickness……...31

3.5: Trends for Varying Leading Edge Radius……..36

3.6: Trends for Varying Maximum Thickness Location……...39

**Chapter 4: Optimization……46**

4.1: Problem Setup……46

4.2.1: Minimizing Lift (Maximizing Downforce)……48

4.2.2: Minimizing Lift Analysis……50

4.2.3: Other Design Considerations……...54

4.3: Minimizing Drag/Lift to Drag Ratio……...55

**Chapter 5: Conclusion and Future Studies……...58**

5.1: Conclusion…….....58

**References……60**

**Appendix A……...62**

## List of Figures

1: final mesh for validation……10

2: airfoil boundary layer mesh……...10

3: ground boundary layer mesh……..10

4: final mesh for geometry study……...11

5: validation of lift values……..11

6: validation of drag values……12

7: validation of lift to drag values……..12

8: percent changes in lift for all geometric parameters……..18

9: percent changes in drag for all geometric parameters……...19

10: percent changes in lift to drag ratio for all geometric parameters……...21

11: percent changes in aerodynamic performance for varying maximum camber……22

12: pressure contours for varying maximum camber……23

13: velocity contours for varying maximum camber…….24

14: pressure distribution for varying maximum camber……25

15: percent changes in aerodynamic performance for varying maximum camber location……..27

16: geometry comparison for extreme aft camber location……...28

17: pressure contours for varying maximum camber location……...29

18: pressure distribution for varying maximum camber location……..30

19: percent changes in aerodynamic performance for varying maximum thickness…….32

20: pressure distribution for varying maximum thickness…….33

21: velocity contours for varying maximum thickness……..34

22: pressure contours for varying maximum thickness…….35

23: percent changes in aerodynamic performance for leading edge radius……...37

24: pressure distributions for varying leading edge radius……38

25: percent changes in aerodynamic performance for varying maximum thickness location…...40

26: pressure distribution for varying maximum thickness location……...42

27: pressure contours for varying maximum thickness location……...44

28: carpet plot for maximizing downforce……49
29: pressure distributions for maximizing downforce……...51
30: velocity contours for maximizing downforce……..52
31: pressure contours for maximizing downforce……53
32: wake analysis for maximizing downforce……...54
33: carpet plot for minimizing drag……...56
34: representation of varying maximum camber……...62
35: representation of varying maximum camber location……63
36: representation of varying maximum thickness……64
37: representation of varying leading edge radius……64
38: orientation of pressure distribution with inverted airfoil……65
39: velocity contours for varying maximum camber location……...65
40: velocity contours for varying leading edge radius……...66
41: pressure contours for varying leading edge radius……..66
42: velocity contours for varying maximum thickness location……66

## List of Tables

1: breakdown of modified NACA Four Series……..14

2: key results from single parameter studies…….17

# Chapter 1: Introduction

## 1.1: Introduction

Formula 1 racing is a competitive, world renowned sport that brings in more than a billion dollars annually [1]. In order to stake a claim in the industry, teams must remain competitive by taking advantage of any performance gains at their disposal. One topic of interest is the understanding of aerodynamics in the design of a formula race car.

In the same way aerodynamics is used to lift an aircraft, this concept can be used to push a car to the ground known as downforce (negative lift). By implementing aerodynamics, the vehicle can experience significantly higher speeds through the turns due to the increased traction [2]. High performance race cars can produce more than three times their own weight in downforce, and record lateral forces of over 3 g's going through turns [2, 3]. However, the incorporation of aerodynamics into racing began simply in the 1960's by using rectangular wings flipped upside down to produce the necessary downforce to allow for higher turning speeds. Ever since these early ventures, aerodynamics has been at the forefront of high performance automotive racing technology. Despite the decades of development for race car aerodynamics, and wings in particular, there is very little in the public domain that is available on the design of automotive aerodynamics. While that is not to say that the subject is unstudied; there is very little available that provides perspective for a wing to be implemented in a Formula or Indy car.

A series of studies was conducted on the effects that near ground proximity had on the aerodynamics of a wing. Since most of the car is in extreme ground proximity, studies of ground effect shed some light on the aerodynamics that would be experienced by race cars. Ahmed et al did a series of studies on wings in ground effect focusing on the potential development of wing

in ground effect (WIG) aircraft. These investigators performed studies on several NACA airfoils (0015, 4412, 4415) and noted that ground effect enhanced the lifting forces of an airfoil even when in extreme ground effect [4, 5]. However, these studies used a flat plate to represent the ground as opposed to a moving belt. Upon retesting the 4412 airfoil with a moving belt to simulate a rolling road, it was found that in extreme ground effect and low angles of attack, the airfoil actually saw a drop in lift [6]. Despite the discrepancies in these studies, it was found that in the case of extreme ground effect and low angles of attack (height/chord [h/c] less than 0.2 and angles of attack from 0-2 degrees), the surface near the ground began to experience a suction effect. This was attributed to the development of a convergent-divergent passage between the airfoil and the ground. Even though this was documented as the cause for the decrease in lift, no studies were carried out to determine the implications of any change to the geometry of this passage. Although these studies encompassed three airfoils from the NACA Four Series family of airfoils, there was no direct comparison made on the general impact the geometry of the airfoils had on the interaction with the ground.

The suction effect due to the convergent divergent passage on the lower surface of the airfoil is what makes the front wing of a race car so effective. Ranzenbach and Barlow performed a series of experiments on an inverted airfoil in ground effect. Using an adjustable flat plate to represent the ground clearance; they discovered that in extreme ground proximity the downforce produced by an inverted airfoil was augmented. Eventually a maximum was reached at approximately 8% chord or 0.08c ground clearance. After that point, the airfoil experienced a rapid decrease in the downforce that was produced. The researchers predicted that this rapid decay could be attributed to the boundary layer convergence between the airfoil and the ground

[7-9]. This boundary layer convergence was later refuted as the reason for the decrease in lift due to studies by Zhang and Zerihan [10].

In Zhang and Zerihan's study of a Tyrrell-26 airfoil, a derivative of a NASA GA(W) profile, they used a moving belt to simulate a rolling road instead of a flat plate. Even with this difference, they still had similar results to that of Ranzenbach and Barlow. Below a ride height of 0.2c, the airfoil saw large increases in the downforce produced with only minor decreases in the ride height. It was this region that they dubbed the force enhancement region. Just as Ranzenbach and Barlow had discovered, at approximately 0.08c ride height, a peak downforce was obtained followed by a sharp decrease which they designated as the force reduction region. Despite finding a similar result, they concluded that the cause of the force reduction region developing was due to an adverse pressure gradient leading to the airfoil stalling and not boundary layer convergence. It was this finding that explains the discrepancy for the results of the second experiment done by Ahmed on the NACA 4412 airfoil. Similarly to Ahmed though, there was reference to a change in the geometry, albeit the actual airfoil itself instead of the passage between the airfoil and the ground. Zhang and Zerihan noted that the modifications to the NASA GA(W) profile to get the Tyrrell-26 airfoil were for wake reduction. Despite mentioning the change in geometry, there were no direct comparisons done to determine if there were any changes to the aerodynamic forces acting upon the airfoil due to these changes.

Yet, geometry changes in airfoils have been studied since the very beginning of flight with the Wright brothers, eventually leading to the establishment of the National Advisory Committee for Aeronautics (NACA) who developed many of the baseline airfoil families that are now used in industry today. Several families of airfoils were developed by this committee with

one family in particular focusing heavily on the geometric characteristics of the airfoil, the NACA Four Series. It was this series that Ahmed et al utilized in their ground effect studies.

The NACA Four Series is identified by four digits defined by three geometric parameters: the maximum camber (first digit), the location of maximum camber (second digit), and the maximum thickness (third and fourth digit). There is also a modified version which is indicated by a dash and two more digits indicative of two more geometric parameters the leading edge sharpness (fifth digit) and the location of maximum thickness (sixth digit). Classical studies have been done on the original Four Series to determine the effects that geometry had on the aerodynamic forces produced by the airfoil. Abbott and von Doenhoff list a series of data sets from various experiments done on the original Four Series. Experimental data, as well as thin airfoil theory shows that increasing the camber of an airfoil will linearly increase the lift produced until the airfoil begins to undergo stall. They also note that increasing the thickness of a symmetric airfoil will also increase the maximum lift produced by the airfoil [11]. This is even referenced by Katz when discussing the design of wings for implementation on race cars [12]. Yet, the results listed by Abbott and von Doenhoff also reveal that the maximum lift coefficient begins to favor thinner airfoils as the camber increases. In spite of this, there were no studies reported that specifically showed the effects of adjusting camber and its distribution, or any of the effects of thickness on highly cambered wings. So any coupling effects that might occur were not specifically listed outside of thin airfoil theory despite the thickness or lack thereof playing a role in improving the performance of the airfoil. This is especially troublesome when considering the data sets did not decrease thickness below 0.09c despite the trends for the NACA 4412 clearly showing a bias in performance toward being even thinner. All in all there is a plethora of data available for the effects of geometry on airfoil performance, but there is a lack of

information of how these geometric characteristics would change when an airfoil is in near ground proximity like that on the front wing of a Formula or Indy car.

There is a great deal of information available on the modification of race car wings through flaps and other high lift devices [12, 13-16]. However, all of this focuses on improving the wing as it already exists. None of the information available discusses the development and design of a wing for race car applications. This cannot be any better highlighted than by a quote from Dominy in which he states that "although some manufacturers have designed aerofoils specifically to operate close to the ground many have simply adopted 'textbook' design" [2]. But, there is very little, if any, information available on the development of these airfoils designed specifically for race cars. Therefore, the goal of this study is to determine the effects of a few design aspects of a classical airfoil family with respect to its utilization in conditions for a race car. Then, use the information gathered and implement classic graphical optimization techniques to further study the relationships between the geometric parameters of the airfoil with respect to important performance criteria.

# Chapter 2: Methodology

In this study, the effects of geometry on the aerodynamic forces acting upon an inverted wing in ground effect were investigated. Due to the range of geometries required for testing in this study, a computational analysis was considered the most practical method to achieve these goals.

## 2.1: ANSYS FLUENT

ANSYS Fluent, a Reynolds averaged, Navier-Stokes (RANS) based solver, was used to simulate the conditions of wind tunnel testing. A baseline data set was selected to understand various model changes. Unfortunately, the data primarily used for inverted wings in ground effect was not readily available, so a study on a non-inverted NACA 4412 in ground effect was selected as the baseline [6] to validate the solver.

### 2.1.1: Turbulence Models

Each turbulence model available in ANSYS Fluent was considered for this investigation. Through a review of the literature [17], and the considerations for testing the most sufficient model was the transition k-kl omega model. While this model does not have a built in adjustment for skin friction, its ability to handle adverse pressure gradients and to predict flow separation were considered ideal. Zhang et al attributed these adverse pressure gradients as the main reason for a reduction in downforce and increase in drag in extreme ground effect [10]. Despite this turbulence selection, the model suffered from convergence issues, in which the end values oscillated. These convergence issues were due in part to the model's prediction of flow separation at the trailing edge of the airfoil producing vortex shedding. While this affected the

convergence of the model, the average of these oscillations was taken, and proved to be accurate within 10% of the experimental data for the computational baseline.

It should be noted that several computational studies have been performed on the experimental data collected by Zhang and Zerihan which resulted in varying turbulence models being considered the most accurate [18, 19]. Due to this confliction, all of the turbulence models listed in the literature were tested as well and each resulted in deficiencies in performance of various parameters. It is these discrepancies that require a more robust computational model to be developed. Instead, one model was selected that allowed for trends to be obtained with reasonable confidence for this design investigation.

2.1.2: Mesh

The size of the domain for testing was chosen as five chord lengths tall and five chord lengths in front of the leading edge of the airfoil. Any decreases in size yielded a decrease in accuracy, while any increases resulted in negligible improvements, but significant increase in computational time. The volume was also eleven chord lengths behind the leading edge of the airfoil to give approximately ten chord lengths behind the airfoil to show the development of the wake. While a thorough investigation of the wake development is not the primary focus of this study, it is an important consideration for race car design, as the car will always lie in the wake of the front wing, so several images in this study will show the wake region along with a brief discussion.

A hybrid structured and unstructured mesh was used to develop an appropriate element concentration in the boundary layer region, while providing a decrease in computation time in the far field. While a complete quadrilateral mesh yielded increased accuracy to the solution,

ANSYS' meshing tools were not robust enough to generate a mesh successively if any changes were made to the model.

When developing the boundary layer for the model, the concentration of elements near the wall play a significant role in the accuracy of the solution. This is especially so in the case of the k-kl omega turbulence model, as it is highly sensitive to the mesh resolution in areas where transition and flow separation are supposed to occur. The value of y+, a dimensionless quantity measuring the height of the first layer from the wall [17, 20] was used to effectively determine the appropriate first layer height. The calculation for y+ can be seen in Equation 1 below,

$$y^+ = \frac{u_* y}{\nu} \qquad \text{(eq. 1)}$$

where y is the height of the first layer, ν is the kinematic viscosity of the fluid, and $u_*$ is the friction velocity at the wall. In the ground boundary layer, a y+ on the order of 10 was used. Lower values of y+ were tested but yielded negligible improvement to the overall model, and merely increased computational time. A y+ value on the order of 0.1 was used for the boundary layer around the airfoil. Values on the order of 1 and 10 were tested, but yielded convergence issues in later iterations and a significant drop in accuracy. Attempts were made to test y+ values lower than 0.1, but issues occurred in the meshing of the boundary layer, resulting in the mesh failing to generate.

Around the airfoil, the boundary layer was designed to be twenty elements thick to allow for appropriate boundary layer thickness and to capture the effects of transition. Increasing or decreasing the number of elements in the boundary layer lead to either decreased accuracy or the mesh failing. However, the boundary layer was meshed using FLUENT's smooth transition feature to allow for the boundary layer to mesh properly for extreme changes in geometry to the

airfoil. This led to varying sizes in the boundary layer in the vicinity of extreme changes in curvature giving a higher concentration of elements in areas most likely to be affected by adverse pressure gradients which was needed for testing changes in the geometry later. In comparison to Ahmed's results, the effects appeared to be minimal, but that study does not take into account varying airfoil geometry. It should be noted that the smooth transition was not sufficient at the trailing edge of the airfoil, and that the trailing edge of the airfoil was modeled with a spline, which allowed for proper wrapping around the trailing edge. The radius of this curvature was less than 0.1% chord, though, resulting in negligible effects on the overall geometry, but it gave significant improvement to the results and modeling of the flow. Without this modification, highly skewed elements developed at the trailing edge of the airfoil, and reversed flow would begin to develop and propagate upstream on both sides of the airfoil resulting in the simulation failing.

### 2.1.3: Final Model

The final result was a mesh of roughly 135,000 elements with an average aspect ratio of 2.64 and an average skewness of 0.0647 displayed in Figures 1-4 below. A recommendation is to have an aspect ratio, or the ratio between the distance from the center of the cell to the nodes and the distance from the center of the cell to the middle of the midpoint between nodes, no greater than 5:1 with an exception to the boundary layer which can approach ratios of 10:1 [17]. In regard to skewness, or rather the difference between the element shape and that of an equilateral element of equal area, it is recommended not to have an average skewness in excess of 0.33 with no single element exceeding 0.95 [17]. Given these recommendations, the quality of the mesh well exceeded these conditions.

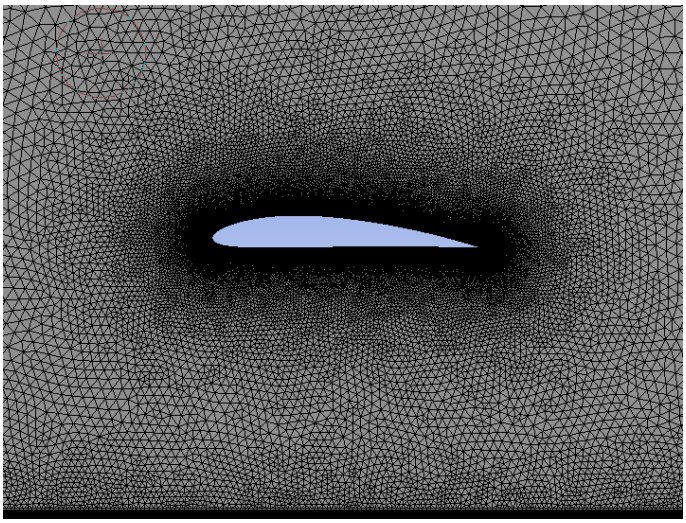

*Figure1: final mesh applied to the NACA 4412 at 2 degrees angle of attack for comparison to Ahmed's data*

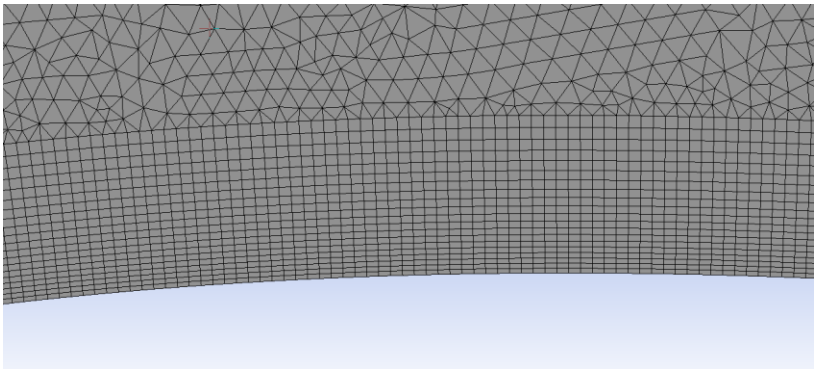

*Figure 2: boundary layer for the NACA 4412 airfoil*

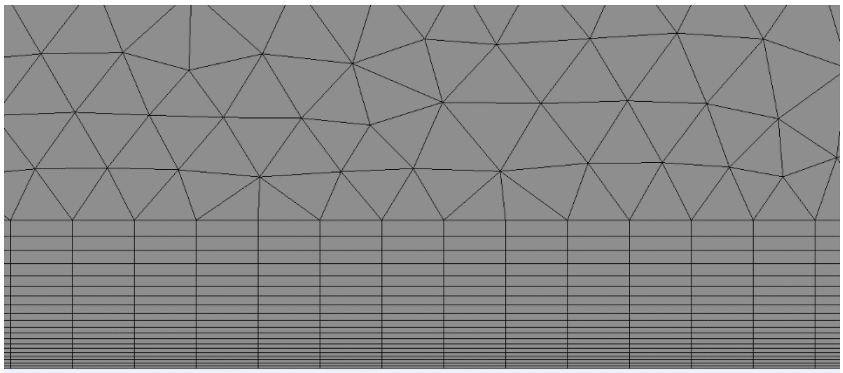

*Figure 3: boundary layer for the ground*

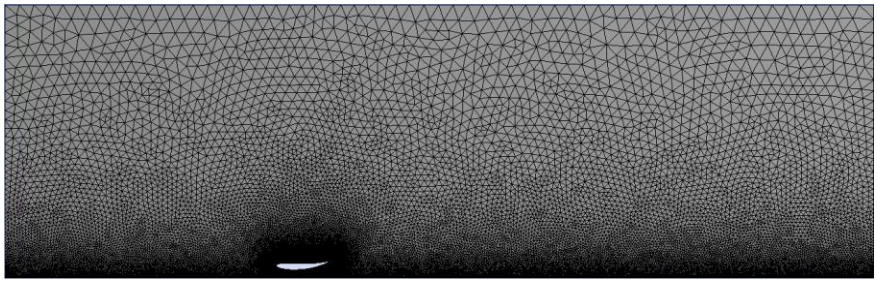

*Figure 4: full domain for inverted NACA 6612 airfoil study*

As stated previously, the model was capable of predicting the results reported by Ahmed to ~10% accuracy, but the most important aspect of the model though, was that it effectively followed the trends of the comparison study displayed in Figure 5-7.

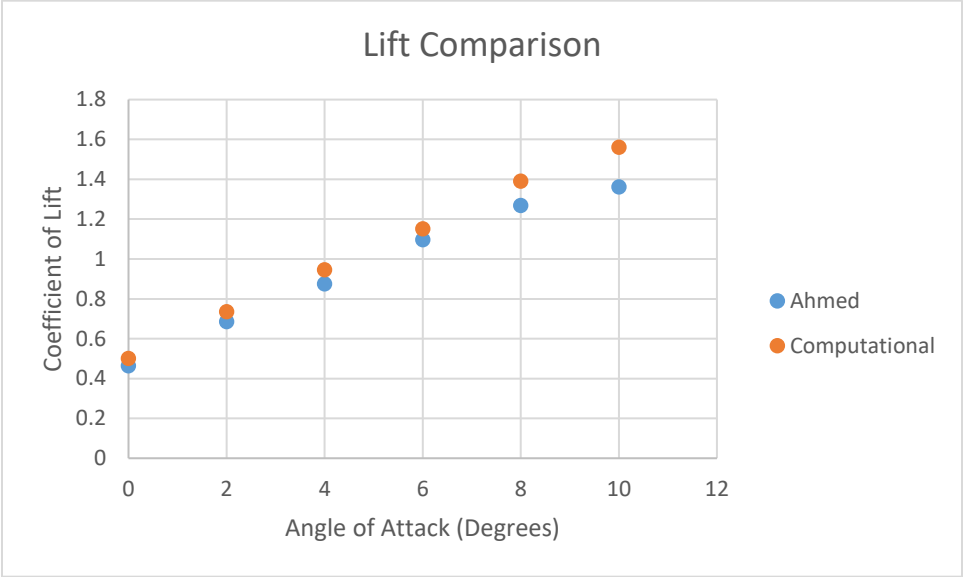


*Figure 5: comparison of lift coefficient for a NACA 4412 airfoil at a height of 1 chord*

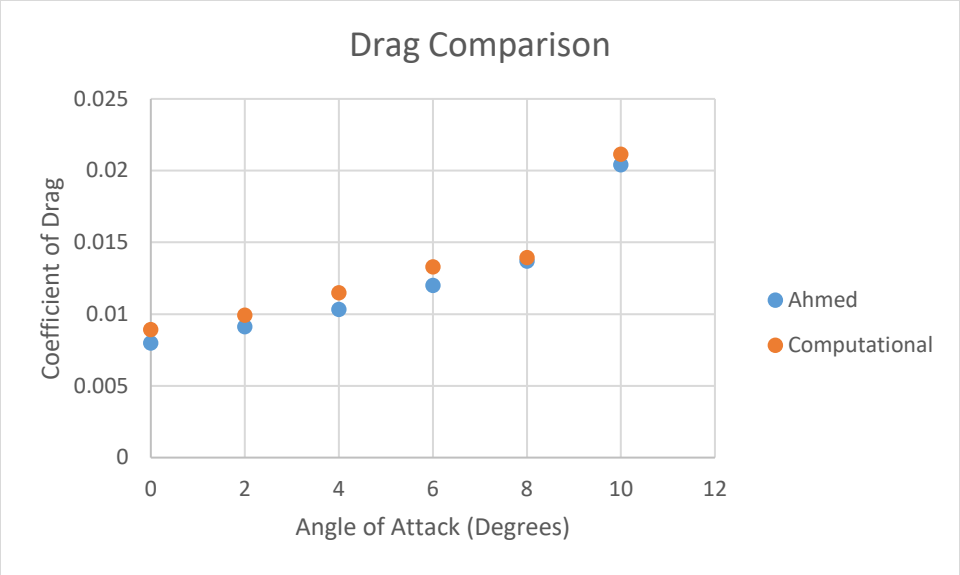


*Figure 6: comparison of drag coefficient for a NACA 4412 airfoil at a height of 1 chord*

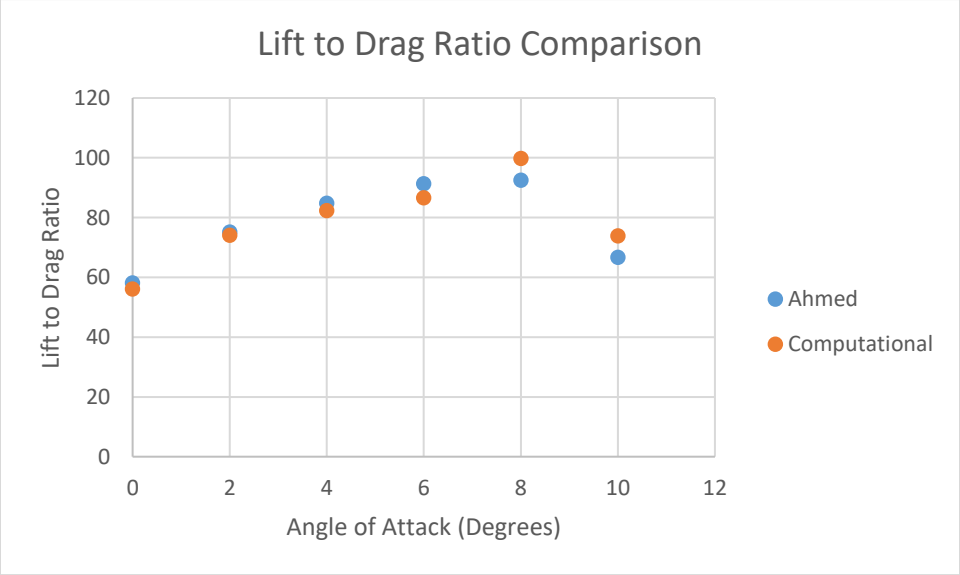


*Figure 7: comparison of lift to drag ratio for a NACA 4412 airfoil at a height of 1 chord*

The flow conditions were that of his testing of the NACA 4412 with a velocity of 30.8 m/s, a chord length of 0.15 m, a Reynolds Number of $3.0 \times 10^5$, and a rolling road at freestream velocity. The model showed flow separation beginning at a similar angle of attack and location on the airfoil, as well as proportional changes in the aerodynamic forces produced. However, when focusing on the delta values between each of the points for determining the general trends,

at zero degrees angle of attack, the computational model under-predicted the change in drag. This is caused by the model being unable to accurately predict changes in skin friction drag which is considerably more important at low angles of attack when pressure drag is low. While the model predicted transition well, once stall began to occur, it resulted in a larger drop in lift and a larger change in drag than were actually reported by Ahmed. For this experiment, this was considered sufficient, as the model accurately predicted the geometric configuration that would yield stall conditions.

### 2.2.1: Set-Up

From the results of the comparison of the NACA 4412 study, it was determined that an appropriate angle of attack would be five degrees. This avoided the insufficiencies in modeling airfoils in the case of low pressure drag, as well as the early onset stall characteristics. A ride height of fifteen percent chord was selected based on the findings of Zhang and Zerihan [10, 15]. Such a ride height was well within the force enhancement region, but it was sufficiently distanced from the force reduction region to avoid stalling effects. Testing in this region would allow for the effects of extreme ground effect that are utilized in the automotive racing industry to be implemented accordingly, and it would allow for a clear baseline model to be developed for geometric design characteristics of race car wings.

### 2.2.2: Procedure (Single Variable Geometry)

To allow for appropriate geometric changes, the NACA Four Series with two digit modification airfoil family was selected for testing. This airfoil family is defined by five geometric parameters, yielding five independent variables, which can be determined by the designated NACA number.

The first digit in the designation number indicates the maximum camber, or maximum curvature of the average thickness line, of the airfoil in percent chord, while the second indicates the location from the leading edge of the airfoil that this maximum camber occurs in tenths of chord. The third and fourth digits of the designation number indicate the maximum thickness of the airfoil in percent chord. A dash follows these four digits, indicating that the airfoil is not a standard Four Series, but has the two digit modification. This fifth digit indicates leading edge sharpness, which is directly related to the leading edge radius [11, 21]. Finally, the sixth digit gives the location of the maximum thickness of the airfoil in tenths of chord from the leading edge. Table 1 gives an example of this below.

*Table 1: NACA Index number relations to geometric parameters*

| **NACA 6612-63** | |
|---|---|
| Digit 1: 6 | Maximum Camber: 6 percent chord |
| Digit 2: 6 | Maximum Camber Location: 6 x 10 (60) percent chord from leading edge |
| Digits 3/4: 12 | Maximum Thickness: 12 percent chord |
| Digit 5: 6 | Leading Edge Sharpness: 6 (radius of 1.5867 percent chord) |
| Digit 6: 3 | Location of Maximum Thickness: 3 x 10 (30) percent chord from leading edge |

For testing, a baseline of the NACA 6612-63 was selected, and each geometric parameter was changed independently while all of the other parameters were held constant. A representation of these changes can be seen in Appendix A. Camber was observed over the range of 0-12 percent chord in intervals of 2 percent chord. The location of maximum camber was tested at 40, 60, and 80 percent chord. Maximum thickness was changed at intervals of 3 percent chord from 3-18 percent chord. While changing the maximum thickness, the leading edge radius was varied with the thickness due to the relation between the two [21], but the designated NACA digit for the leading edge remained constant throughout. In testing the effects of the leading edge

radius had on aerodynamic forces, the radius was varied with respect to the designated NACA digit from 2-14 in intervals of 2. Maximum thickness location was varied from 10 percent chord in intervals of 10 percent chord until 60 percent chord. The resultant changes in aerodynamic forces with respect to the baseline were recorded and interpolated to create trend-lines for comparisons between the impacts of each geometric parameter on the desired performance of the airfoil for race car wing development. Further testing was done within these sets to get close to local maxima in downforce for design consideration which will be discussed later on in the next chapter.

### 2.2.3: Generation of Airfoil Coordinates (JAVAFOIL)

In order to effectively change all of the geometric parameters successfully and input the airfoil geometries into FLUENT, the equations that define the NACA 4 Series with two digit modification [11] must be used to define the appropriate coordinates of the airfoil. Through various studies of these equations, computer programs have been created in which the NACA index number can be input, and the appropriate coordinates for that particular airfoil can be output [21]. For this study, the program JAVAFOIL was used due to its accuracy and ease of use.

Using coordinates from NACA [11], the coordinates produced by JAVAFOIL were compared to measure accuracy. The results were nearly identical with the only coordinates having a large percent error being near the trailing edge where the corresponding y-values are small so the difference was insignificant. The program was considered within satisfactory tolerance for the investigation.

In generating the airfoil coordinates, JAVAFOIL successfully generated all of the required geometric configurations needed for this study. However, it should be noted that for the

leading edge radius, the equations that determine the airfoil coordinates were considered inaccurate for a NACA index number greater than 8 [11]. While JAVAFOIL successfully generated coordinates for airfoils with a leading edge radius of appropriate size corresponding to the NACA index number, it is unknown whether these airfoils are an accurate representation of the NACA 4 Series family of airfoils. This is due to either the inaccuracy of the equations, or constraints to the airfoil family itself. Further studies need to be conducted to either develop a more accurate program, or develop an appropriate airfoil family, as no references to airfoils with a NACA Index number greater than 8 are listed in any references found.

For the generation of the maximum thickness location, a note should be made that any maximum thickness location further back than 60 percent chord led to inaccurate geometries in JAVAFOIL due to a lack of constraints on the trailing edge angle. However, this limitation did not impact the necessary results acquired from testing, but it did hinder particular aspects of the discussion.

### 2.3: Single Variable Trends

Once the tests were completed, and the data were interpolated. The local maxima yielded were then used as testing points to find the maxima in downforce for each geometric parameter. Each maxima was tested, and the results reviewed until an appropriate maxima was obtained for each geometric parameter. This gave a clear representation of the potential gains that could be had through the variation of each geometric parameter.

### 2.4: Optimization

For this study, the implementation of carpet plots will be used for determining an optimum design. The ways in which carpet plots can be set up has been well documented in the

references and will not be listed here [22]. By using carpet plots due to their ease of use, the optimization process was limited to two variables. Further discussion on the setup of the optimization and the design considerations that went into it can be found in Section 4.1.

## Chapter 3: Results and Discussion

### 3.1: Single Variable Trends

For this analysis, the modified NACA Four Series family of airfoils was simulated computationally for an inverted configuration within extreme ground proximity to test for the effects of geometry changes. Each of the five geometric parameters was varied independently of the others with respect to a NACA 6612-63 baseline. The aerodynamic forces were recorded, and trends formed from these results were developed to give insight into the design elements of a race car wing. Table 2 shows key points in these trends while Figure 8 below shows the results of the generation of downforce for all of the geometric parameters.

*Table 2: minima and maxima for downforce, drag, and lift to drag ratio for each of the five geometric parameters*

| | | | Maximum Camber | Maximum Camber Location | Maximum Thickness | Leading Edge Radius | Maximum Thickness Location |
|---|---|---|---|---|---|---|---|
| Downforce | Max | Geometric Value | 9 | 95* | 7 | 8.0 | 25 |
| | | Percent Change | +18.3% | +2.97% | +8.44% | +3.88% | +4.46% |
| | Min | Geometric Value | 0* | 40* | 3* | 0.18* | 60* |
| | | Percent Change | -45.2% | -6.94% | -18.4% | -0.69% | -25.0% |
| Drag | Max | Geometric Value | 12* | 95* | 18* | 8.64* | 10* |
| | | Percent Change | +158% | +48.8% | +25.2% | +3.97% | +31.9% |
| | Min | Geometric Value | 0* | 40* | 6 | 7.4 | 60* |

| | | | | | | | |
|---|---|---|---|---|---|---|---|
| | | Percent Change | -54.5% | -3.48% | -20.3% | -0.74% | -17.8% |
| Lift to Drag Ratio | Max | Geometric Value | 2 | 60 | 6 | 7.4 | 25 |
| | | Percent Change | +33.5% | +0.0% | +35.4% | +4.47% | +8.17% |
| | Min | Geometric Value | 12* | 95* | 3* | 8.6* | 10* |
| | | Percent Change | -58.8% | -30.8% | -33.2% | -2.64% | -38.2% |

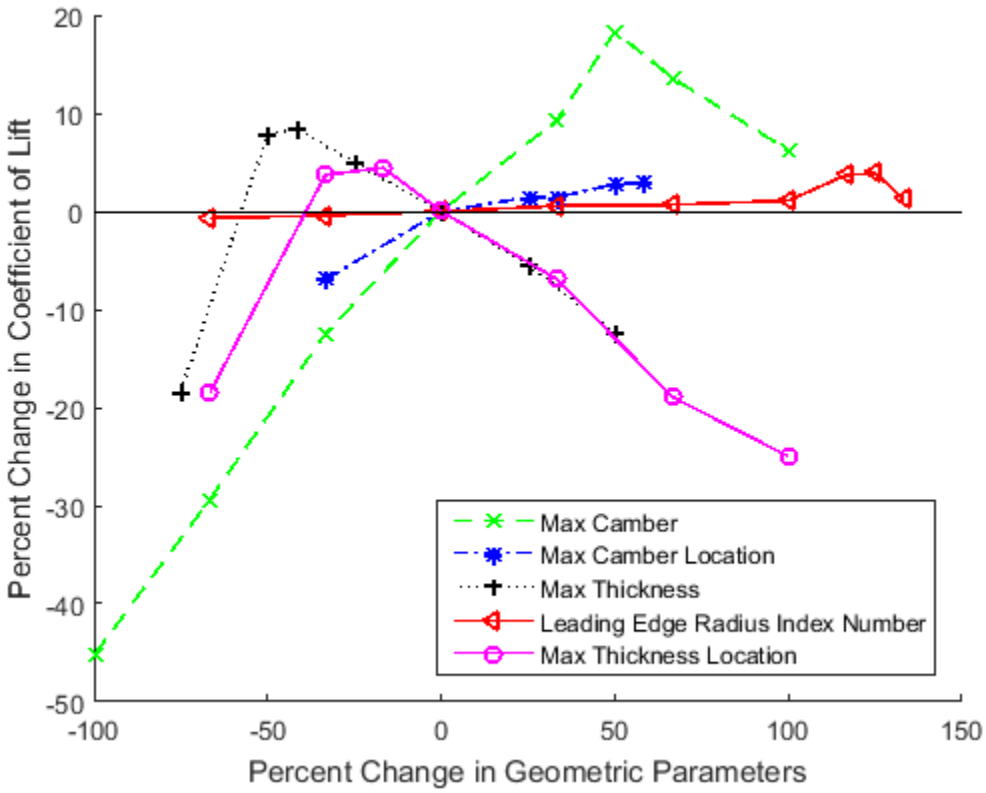


*Figure 8: changes in downforce, normalized as percent changes in downforce with respects to percent change in geometric parameters*

A black line represents zero increase in downforce, thus, all values above that are of interest as the goal of a race car is to produce more downforce. As can be seen from the figure, an increase in downforce can be attained using any geometric parameter. However, the trends are clearly dominated by the maximum camber of the airfoil. The causation of these trends will be discussed

later on in the chapter. A significant feature to note is that changing the leading edge radius yields negligible results in downforce until a certain point is reached in which the downforce production jumps up rapidly then drops just as rapidly. This shows that, if implemented correctly, leading edge radius can introduce a large increase in downforce; although, it is a highly sensitive feature of the airfoil.

The phenomena of a downforce spike for leading edge radius becomes even more intriguing when looking at the trends in drag in Figure 9.

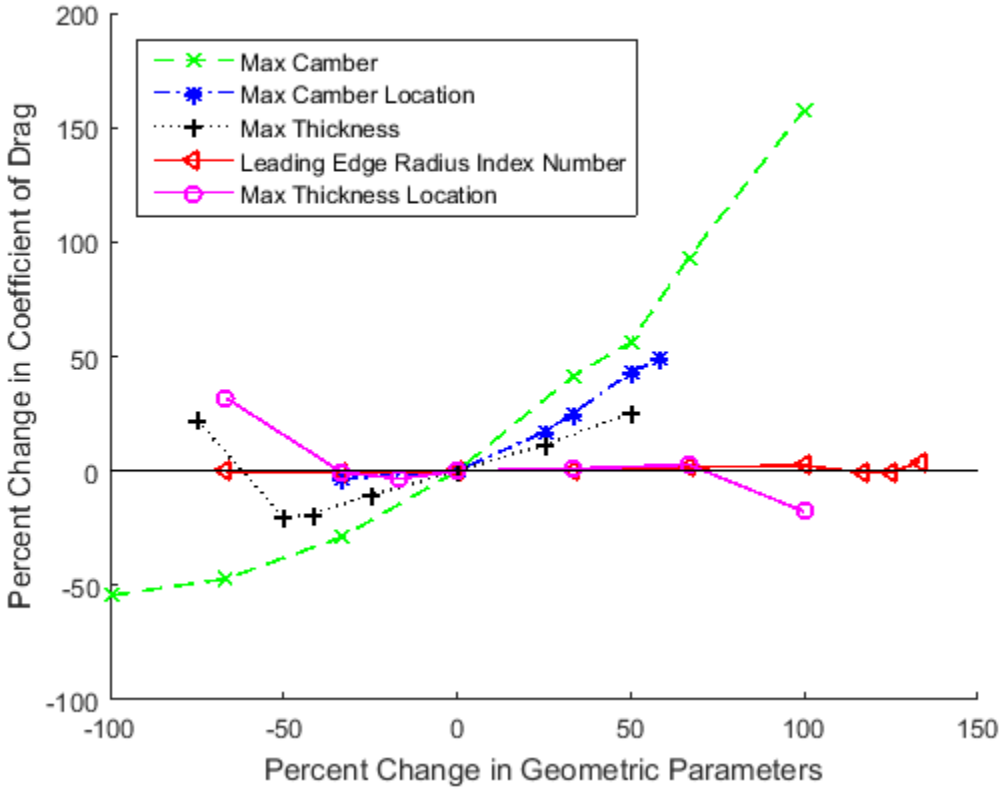


*Figure 9: just as the downforce trends shown previously with drag, except in this instance a positive increase is now of negative consequence*

In the region where the leading edge radius experiences a spike in downforce production the drag actually decreases. Looking at the other geometric parameters, again, camber dominates the overall changes in drag with a large increase in drag as the camber is increased. This means that

while a large amount of downforce is produced when increasing camber, a large amount of drag is produced as well. A similar trend can be seen for changing the maximum camber location; as more downforce is produced, drag increases. Yet, changing the maximum thickness as well as the maximum thickness location has a similar effect to changing the leading edge, producing less drag in regions of increased downforce. Trends like these indicate that while large increases in downforce can be seen from adjusting the camber of an airfoil, this downforce production comes with a large penalty in drag, and thus, a reduced lift to drag ratio as opposed to changing leading edge radius, thickness, or thickness location.

Lift to drag ratio is an important consideration for aerodynamic performance since disproportionate increases in drag can mitigate the benefits of increased downforce. These trends in lift to drag ratio are shown in Figure 10.

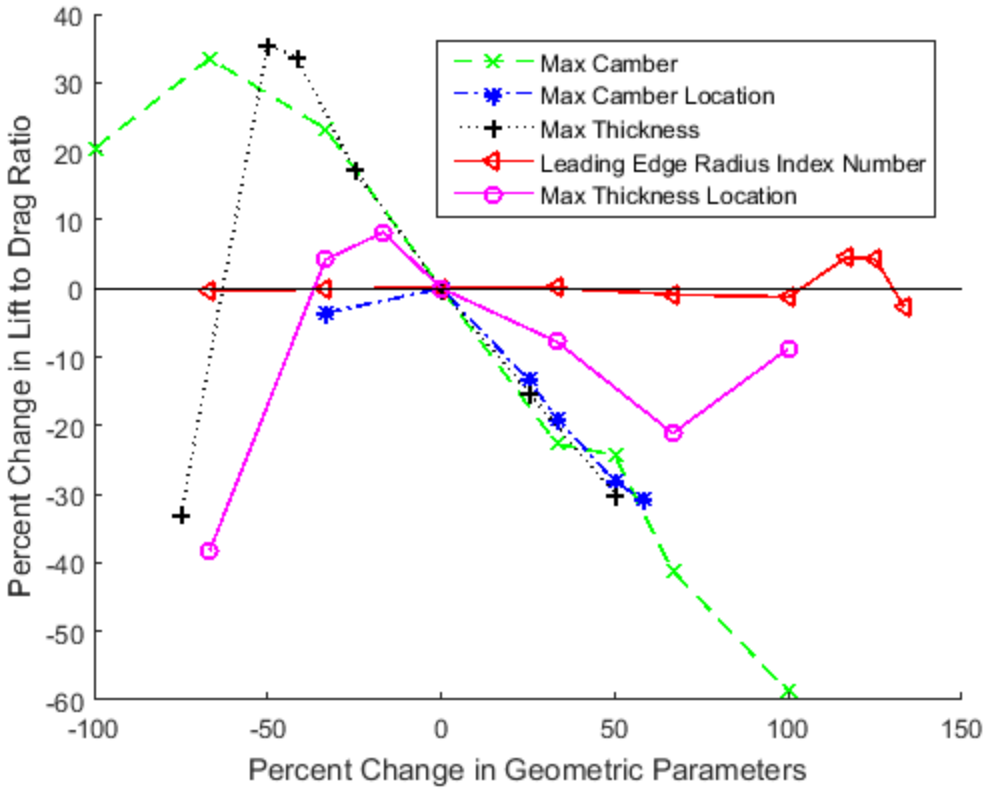


*Figure 10: lift to drag ratio of each geometric parameter, normalized as in the previous figures*

As anticipated, changing the leading edge radius, maximum thickness, and maximum thickness location lead to increases in lift to drag ratio within the regions of increased downforce generation. That indicates that while these mechanisms do not produce the largest increase in downforce, they do produce it without the drag penalties experienced when adjusting camber. Changing the airfoil camber is clearly an effective way to produce downforce; although, it has the most serious drag penalties. In fact, when changing the camber of the airfoil, it produces the highest lift to drag ratios when there is almost no camber at all to the airfoil. While adjusting the location of the maximum camber is not as extreme as changing the maximum camber of the airfoil, it still has an increase in lift to drag ratio outside the region where its biggest gains in downforce would be attained.

3.2: Trends for Varying Maximum Camber

As was shown in the previous section, changing the amount of camber of the airfoil resulted in the greatest changes in the downforce produced; although, it was accompanied by large drag penalties. Figure 11 shows the changes in aerodynamic characteristics relative to the baseline NACA 6612-63.

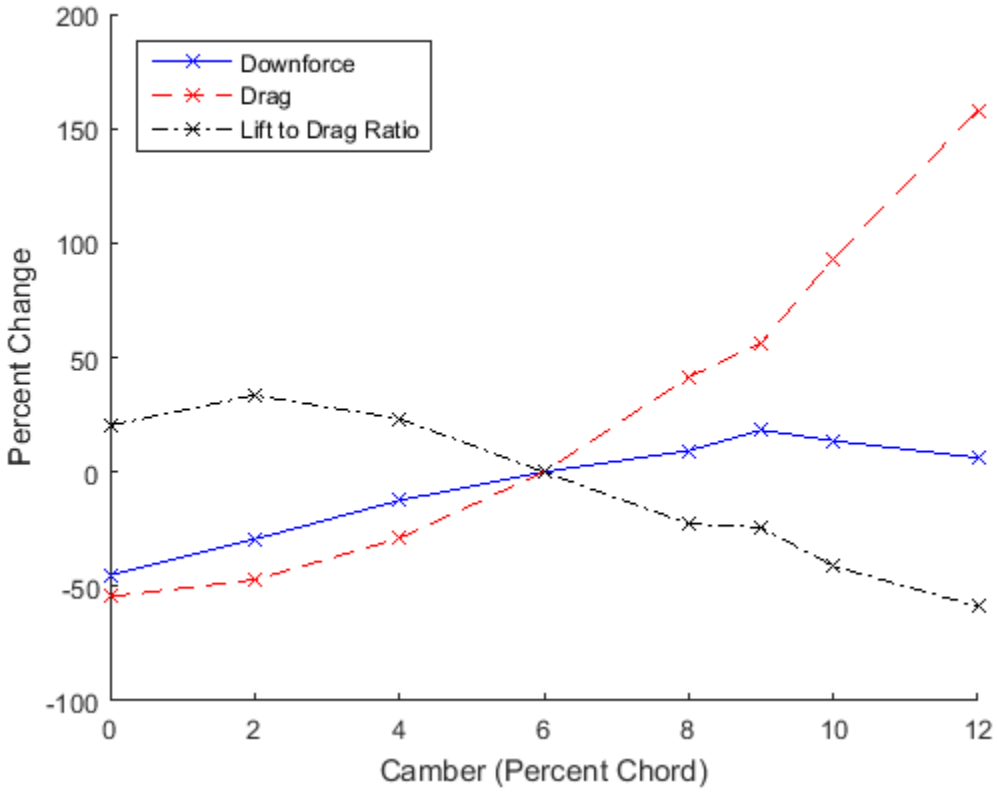


*Figure 11: change in the coefficient of lift, drag, and lift to drag ratio for varying maximum camber*

Looking at the trends in variation of downforce, it can be seen that the largest increase in downforce of 18.3% occurs when the maximum camber is nine percent chord. However, this also comes with a disproportional increase in the drag of over 56%, resulting in a drop in the lift to drag ratio of 24%. That disproportional change in drag appears to be parabolic in nature with increasing maximum camber, and the changes in downforce prior to the maximum camber

reaching nine percent chord are almost linear. Both of these are trends that would be expected based upon thin airfoil theory given that changing the maximum camber changes the zero lift angle of attack of the airfoil, effectively showing what would be expected for a change in the angle of attack itself.

It is the increase in pressure drag from the increased pressure on the upper side of the airfoil illustrated in Figure 12 that results in the disproportional changes in drag.

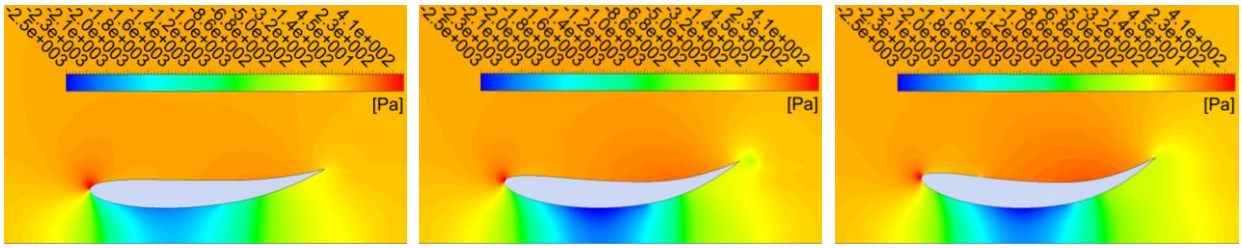


(a) (b) (c)

*Figure 12: pressure contours of the 6612-63 (a), (10)612-63 (b), and (12)612-63 (c)*

As the maximum camber increases, the pressure on the pressure side of the airfoil increases in magnitude as well. But, due to the increase in curvature of the pressure side, the resultant force being applied to the upper surface has a component more parallel to the flow with increasing camber. Yet, the increases in drag from increasing camber are twofold. Figure 13 shows a rapid increase in the flow separation that is occurring near the trailing edge due to the adverse pressure gradient developing on the suction side.

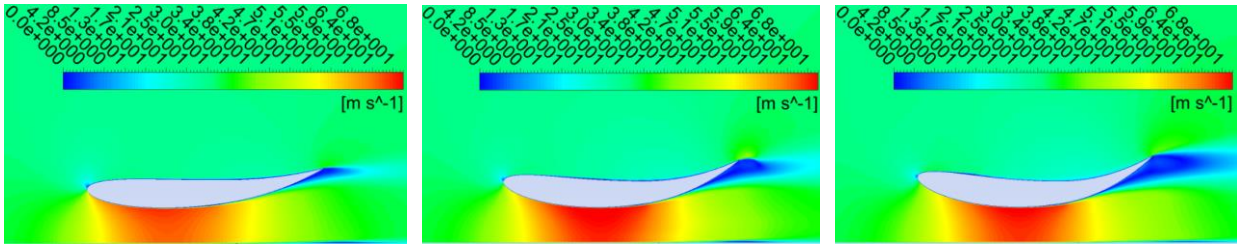


(a) (b) (c)

*Figure 13: velocity contours of the 6612-63 (a), (10)612-63 (b), and (12)612-63 (c)*

It is this coupled effect that shows why a symmetric airfoil produces the lowest drag with a decrease of over 54%. This is due to the lack of pressure build up on the upper side of the airfoil as well as the reduction in flow separation. But that is not to say that this is the most effective way to reduce drag in the airfoil. If downforce is still desired, as well as a high lift to drag ratio, adding a small amount of camber will create more downforce than drag, thus producing a higher lift to drag ratio. Having a camber of two percent chord resulted in an increase in lift to drag ratio of 33.5% while only losing about 30% downforce as opposed to the case of no camber with an increase in lift to drag ratio of just over 20%, but a loss of downforce of over 45%.

Looking at the pressure distributions of Figure 14 it is easy to see why it is that adding camber would cause such an increase in downforce to develop.

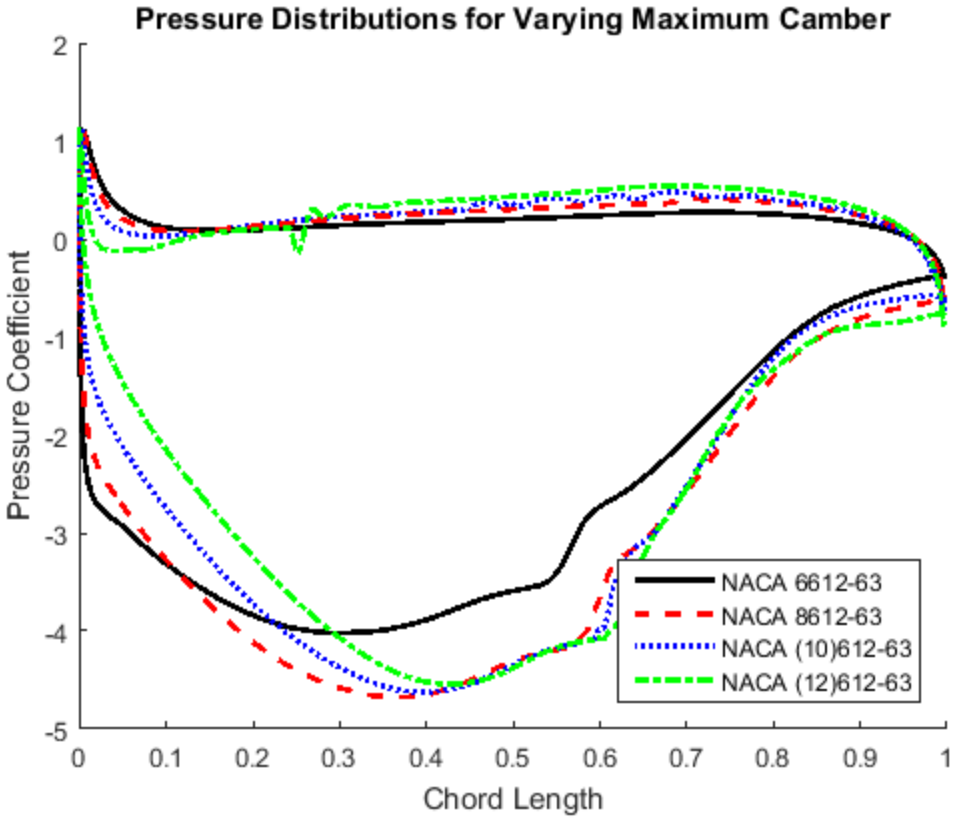


*Figure 14: pressure distributions of four airfoils tested having 6, 8, 10, and 12 percent maximum camber.*

It should be noticed that the orientation of the y-axis in this case is inverted compared to a non-inverted wing. An illustration of the pressure distribution with airfoil orientation can be found in Appendix A. As camber is added, the suction peak on the lower surface of the airfoil increases. Yet, as camber continues to increase, the suction peak moves away from its original location near the location of maximum thickness, and it begins to move toward the location of maximum camber. So, as the suction peak moves further from the location of maximum thickness, it begins to decrease in magnitude. This trend shows that the causation for the peak production of downforce is due to a significantly high suction peak, but one that is distributed over a larger area for the given camber.

So, for a given design space, in order to greatly increase the lift to drag ratio of an airfoil if it is highly cambered, without significant losses to the downforce produced, the camber could be marginally reduced, due to the nature of drag increases with respect to camber. However, if the airfoil is not highly cambered, or even lacks camber, significant downforce can be added just by increasing the camber without sacrifices being made on the lift to drag ratio of the airfoil. Yet all of these depend greatly upon a balance being struck through the curvature of the suction side. Increasing curvature causes an increase in suction peak, but it also decreases the effective area as well as increasing flow separation. Finding the desired characteristics is the key to implementing camber effectively in the development of a race car wing.

### 3.3: Trends for Varying Maximum Camber Location

As was the case with increasing the maximum camber of the airfoil, moving the location of maximum camber further aft on the airfoil resulted in more downforce being created, while also yielding increased drag penalties. Figure 15 shows the aerodynamic trends while varying the location of maximum camber.

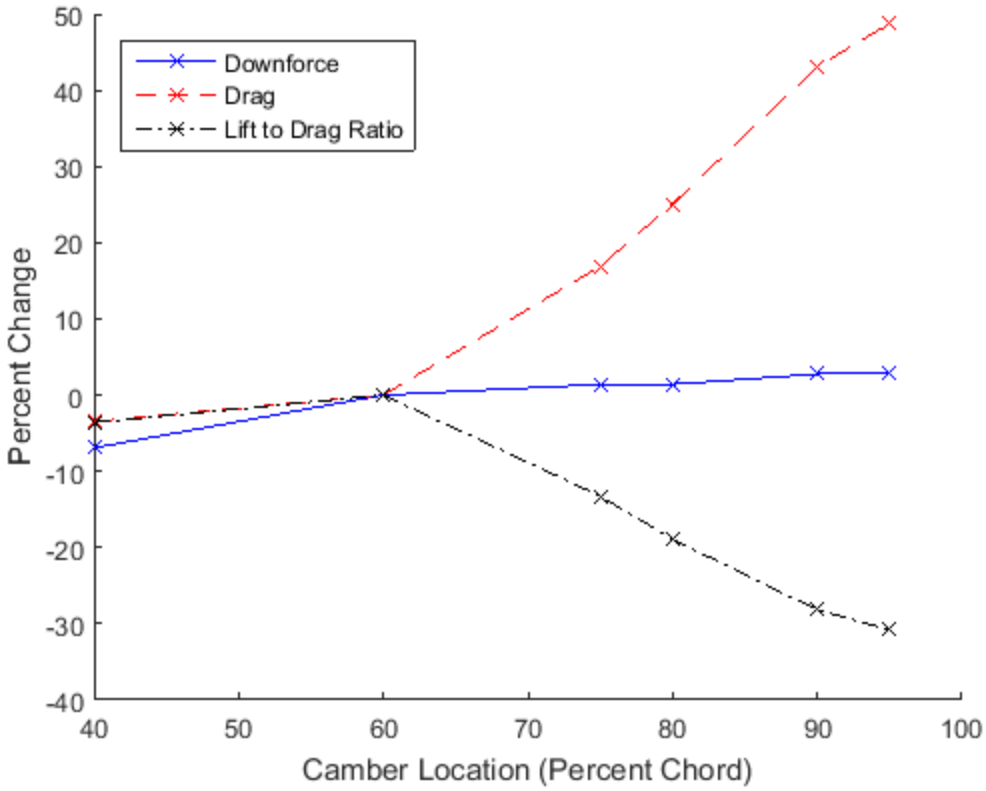


*Figure 15: change in lift, drag, and lift to drag ratio with respect to the location of maximum camber*

Unlike changing the maximum camber, however, thin airfoil theory does not apply. In thin airfoil theory, the trend in lift generated would have increased asymptotically toward infinity as the maximum camber location proceeded to the trailing edge of the airfoil. However, in this setup, the coefficient of lift asymptotically approaches a finite value as it goes toward the trailing edge.

When the maximum camber is located at roughly seventy-five percent chord, there is an increase in downforce over the baseline of roughly 1.4%. Then, the downforce produced remains relatively constant as this location moves further aft. All the while, drag is increasing at a much faster rate yielding increases of nearly 17% resulting in a decrease in lift to drag ratio of over 13%. Yet, downforce increases marginally at eighty percent chord before it continues to climb to

its limit as the maximum camber approaches the trailing edge. At ninety-five percent chord, the maximum camber location yields an increase in downforce of approximately 3%. Again, drag has still increased greatly compared to the downforce by nearly 50% resulting in a loss of lift to drag ratio of over 30%. It is important to note that testing locations further aft resulted in somewhat unreasonable, but useful, airfoil geometries similar to that of a gurney flap shown in Figure 16 below. Although this geometry change looks similar to a gurney flap, it does not act quite like that of adding a gurney flap due to changing the camber distribution without adding further camber.

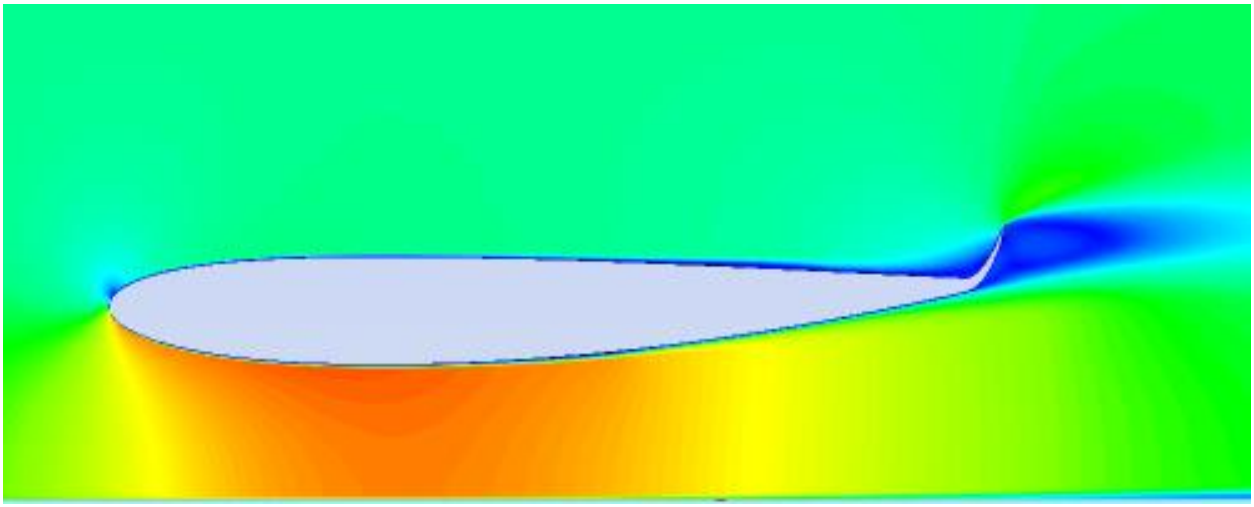

*Figure 16: as the maximum camber location moves near the trailing edge, the geometry resembles that of a gurney flap*

So, unlike increasing the overall camber of the airfoil, moving the location of the maximum camber did not have as significant of an effect on downforce. However, it does still come with heavy drag penalties, even more disproportionate than when increasing the maximum camber. When looking at the seventy-five and ninety-five percent chord locations, the drag increases by approximately 17% and 50% respectively. The reason for these changes in drag is due to the same reason as that for changing the maximum camber; a change in pressure drag on the upper surface illustrated by the pressure contours in Figure 17 below.

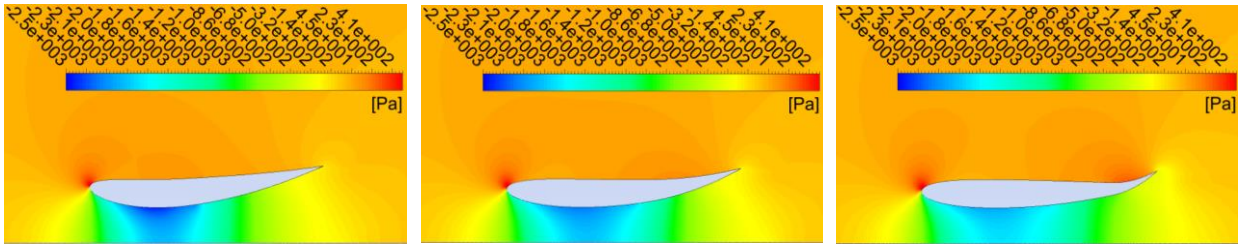


(a) (b) (c)

*Figure 17: pressure contours when changing the maximum camber location from 40% (a), 60% (b), and 80% (c) chord*

Yet, from this figure, if the pressures being applied were like that of changing the maximum camber of the airfoil, then the increase in suction peak would result in higher downforce.

Considering the increase in suction in Figure 17a where the suction peak is, it would be expected that downforce would increase, but that is not the case. Looking closer at the pressure distributions in Figure 18 that downforce is composed of two major parts, the suction on the lower surface and the pressure on the upper surface which did not have a significant effect on downforce previously.

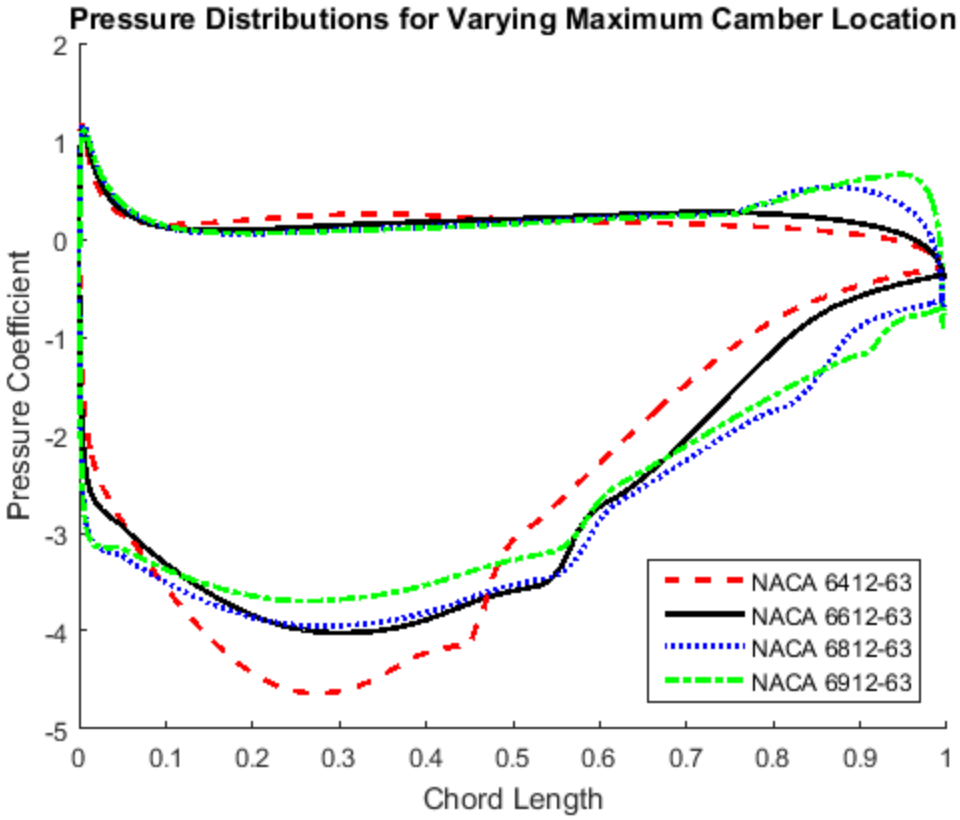


*Figure 18: pressure distributions of airfoils with four different locations of maximum camber*

Similarly to increasing the maximum camber, shifting the maximum camber location aft increases the effective area of the pressure distribution. Meanwhile, moving it toward the maximum thickness location, the suction peak increases in magnitude but decreases in effective area. Yet, what keeps these changes in downforce so stagnant compared to increasing the maximum camber is that flow is reattaching due to the change in pressure gradient with the maximum camber location moving further aft, and the increase in the pressure on the upper surface contributes to downforce as well. This gurney flap type of geometry mitigates the issues of flow separation which plagued the adjustments of maximum camber, but builds a great deal of pressure on the upper side of the airfoil. So, while it definitely affects the amount of drag on the airfoil, the tradeoffs from adjusting camber location are not significant when considering downforce.

These major changes explain why the maximum lift to drag ratio occurs when it does. While downforce can be increased by moving the maximum camber further aft, the drag will significantly increase as well. Also, while the drag can be further reduced by moving the maximum camber forward, it will cause the downforce to decrease. Therefore, that ideal region is where the sensitivity in drag begins to increase at a higher rate while the sensitivity of the downforce begins to decrease. So, there exists a balance not only in the suction side of the airfoil, managing the magnitude of the suction peak with its distribution across the surface, but also in maintaining a high downward component on the pressure side of the airfoil to reduce drag as well.

### 3.4: Trends for Varying Maximum Thickness

In varying the maximum thickness of the NACA 6612-63, the trends differed from those of varying the maximum camber or its location previously. Figure 19 shows the results for these variations.

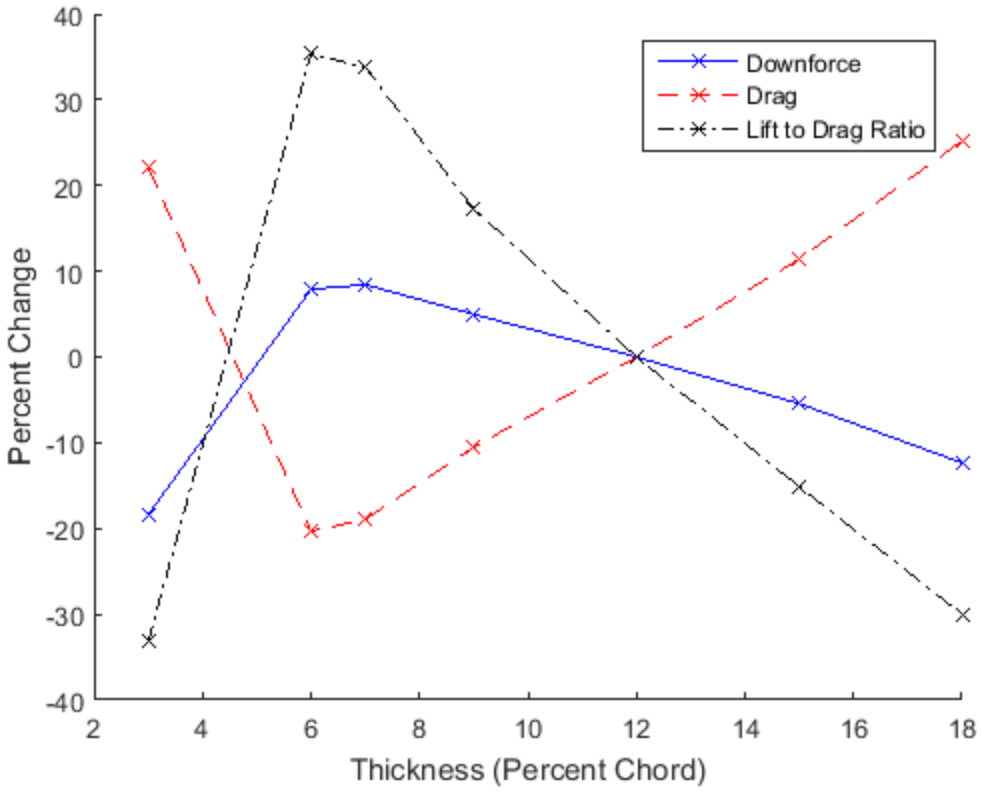


*Figure 19: relationship between downforce, drag, and lift to drag ratio for varying maximum thickness*

Looking at downforce, the general trend is similar to that of varying the location of maximum camber; although, the initial increase from a low value has a much sharper increase in downforce. While, these increases are much more significant than those for varying maximum camber location, they are not nearly as much as those from changing the maximum camber itself. What is significant though, is the large changes that occur when the airfoil is very thin. At approximately six percent chord, the downforce increases by nearly 8 % compared to the NACA 6612-63. These results differ from those reported by Katz [12] for a symmetric wing in freestream, but they correspond well to what would extrapolate from Abbot and von Doenhoff [11]. This sharp drop off in downforce for extremely thin airfoils is caused by a lack of displacement of air, and thus the small changes in the pressure distributions of Figure 20.

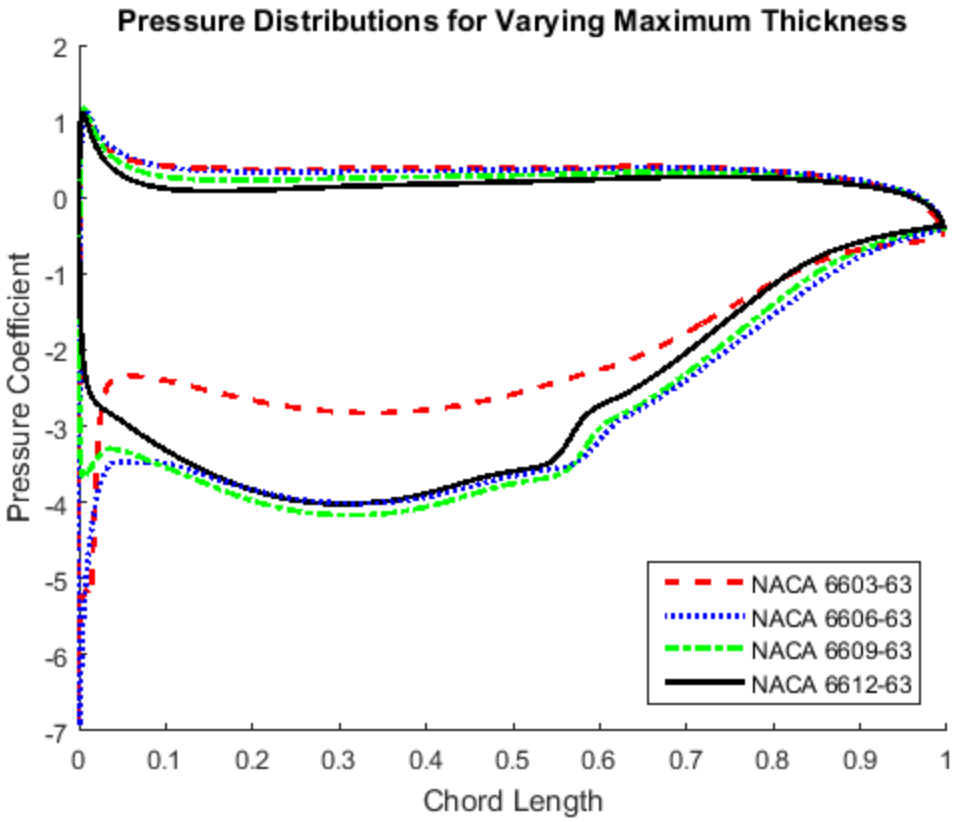


*Figure 20: pressure distributions of four airfoils wither different maximum thicknesses*

As can be seen, there is little variation in the pressure distribution except when the airfoil is extremely thin resulting in a massive drop in suction on the lower surface of the airfoil, except around the leading edge where it increases.

So, changing the maximum thickness can not only increases downforce, but having a maximum thickness which is too thin can actually yield significant decreases in downforce production overall. Unlike adjusting the camber of the airfoil though, drag is affected in a much different manner.

The important distinction between the trends in drag from the previous results is that it follows an almost identical, but opposite trend, as the downforce. So, while changing the maximum camber and its location to increase downforce resulted in increasing drag, changing

the maximum thickness to increase downforce resulted in decreasing drag. The thickness with the minimum drag is at six percent chord. This is the same region for producing the most downforce, or at the very least, in the region with very low downforce sensitivity. Comparing this to the baseline NACA 6612-63 resulted in a decrease in drag of 20%. These large drops in drag, which correspond with large increase in downforce, are due to the general curvature developed by thickness making a more favorable pressure gradient. It is the development of favorable pressure gradients which leads to the reduction of flow separation in Figure 21.

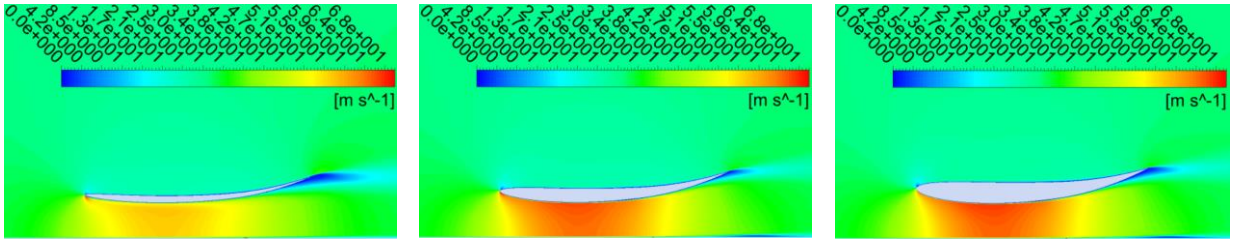


(a) (b) (c)

*Figure 21: velocity contours when changing the maximum thickness from 3% (a), 6% (b), and 9% (c) chord*

By reducing flow separation through the adjustment of the pressure gradient without altering the suction peak, changing maximum thickness results in the highest changes in the lift to drag ratio of any of the parameters observed in this investigation. Comparing this favorable thickness to the baseline case, there was an increase in lift to drag ratio of over 35%. This is because changing the thickness not only increased downforce, but decreased the drag as well.

While it may not seem that adjusting the maximum thickness of an airfoil has any drawbacks given that it can improve downforce and drag simultaneously, there are a few changes to the pressure distribution that could be improved upon. Looking at Figure 22 for extremely thin airfoils there is a high pressure on the upper surface concentrating the resultant net force downward.

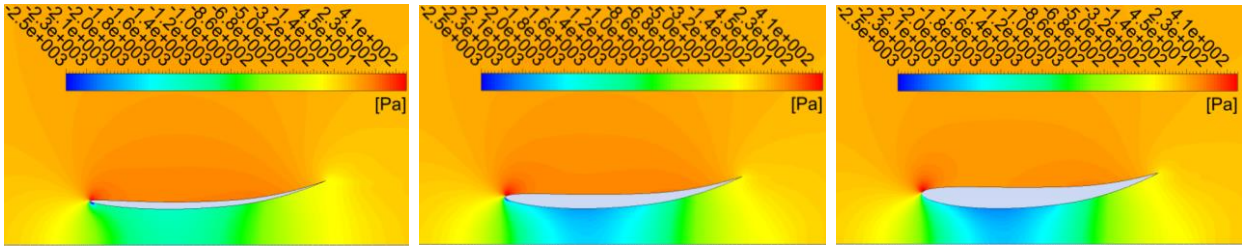


(a) (b) (c)

*Figure 22: pressure contours when changing the maximum thickness from 3% (a), 6% (b), and 9% (c) chord*

But, as thickness is added, the concentration of pressure moves toward the location of maximum camber, which causes the resultant force to have a more parallel component, and increase the drag developed on the upper surface. The general region of high pressure also decreases in area, reducing the effective downforce being developed by the upper surface due to the accelerations over the increased positive-to-negative curvature. However, these drawbacks are mitigated by the positive effects the maximum thickness has on the pressure gradient of the suction side of the airfoil.

Overall, this indicates that changing the maximum thickness of an airfoil can improve downforce while also improving the drag produced by the airfoil. This results in dramatic changes in lift to drag ration, in which minimizing drag, maximizing downforce, and maximizing the lift to drag ratio occurs at almost the same thickness. Changing the thickness appears to be the most ideal way to adjust the airfoil, as any positive change in a particular design parameter results in positive changes to the other performance criteria. This means that it may be utilized with other geometric parameters to augment any one particular performance criteria while potentially reducing the penalties to other criteria. However, the geometry is more complicated.

As thickness is added to an airfoil, more flow is displaced underneath increasing the velocity and the downforce produced. This also decreases the flow separation that occurs at the

trailing edge, thus reducing the drag as well. But, there is a large relationship between the thickness and the camber of the airfoil. The thickness causes the effective curvature on the pressure side to decrease, resulting in higher losses in downforce despite the gains caused by the velocity increase on the suction side. It also causes the pressure to be focused at the location of maximum camber and cause a resultant force that increases the drag. This same effect occurs at the trailing edge in regard to the flow separation, but is even further complicated by the leading edge as well. In order to effectively develop an airfoil, a balance must be found between the curvature of the pressure side as well as the suction side to balance pressure, suction, flow displacement, and flow separation. However, this becomes even more complicated due to the heavy influence of the camber, camber location, thickness distribution, and leading edge radius. Unfortunately, these high-order, intertwining relationships are outside the scope of this study.

### 3.5: Trends for Varying Leading Edge Radius

Unlike any of the previous geometric parameters discussed, changing the leading edge radius leads to highly sensitive changes in the aerodynamic forces acting upon it. However, there are certain features of the trends that resemble some of the previous cases as seen in Figure 23.

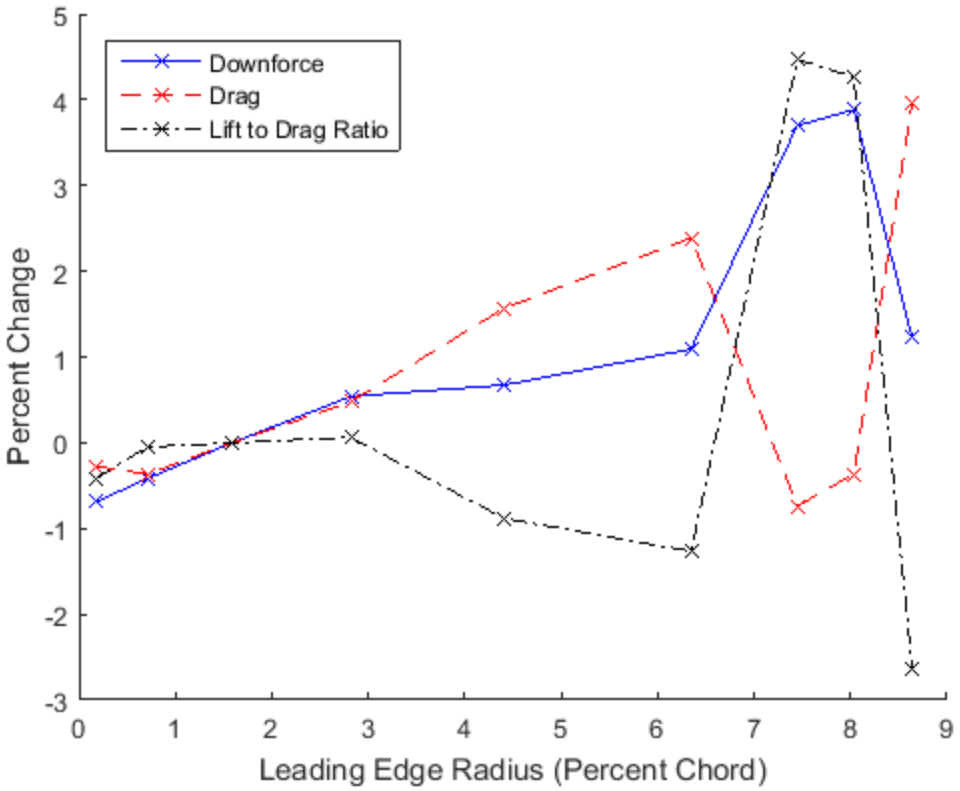


*Figure 23: changes in lift, drag, and lift to drag ratio for variations of the leading edge radius of the baseline NACA 6612-63*

Just like changing the location of maximum camber, there is an initial region that appears to be developing a peak in downforce that does not correspond to the overall maxima of the data set. It does however, correspond to a peak in the change in drag resulting in a valley in lift to drag ratio. Also, there is a region of high sensitivity, near the peak downforce production region, just as there was for changing the maximum thickness of the airfoil; although, it occurs on both sides of the peak.

The initial peak region in the trend line of nearly four percent chord, compared to the baseline of nearly 1.6% chord, results in an increase in downforce of less than one percent. Whereas, the maxima at the actual peak of roughly 7.8% chord resulted in an increase in downforce of four percent. This peak not only shows a larger increase in downforce, but also

shows dramatic sensitivity compared to the rest of the data set. When the leading edge radius is less than six percent chord, the change in downforce is less than 1% compared to the NACA 6612-63. However, the percent increase in downforce from 6.3% chord to 7.4% chord is more than three times greater as it increases from a 1.1% increase to 3.7% increase from the baseline respectively. At the peak, the leading edge radius increases further by less than one percent chord to achieve the maximum downforce increase of nearly 4%. All of this occurs without significant penalties due to drag. In fact, between 7.4% and 8% chord, drag actually decreased compared to the baseline, albeit by less than one percent. The pressure distributions of Figure 24 show that these changes occur primarily on the suction side of the leading edge of the airfoil.

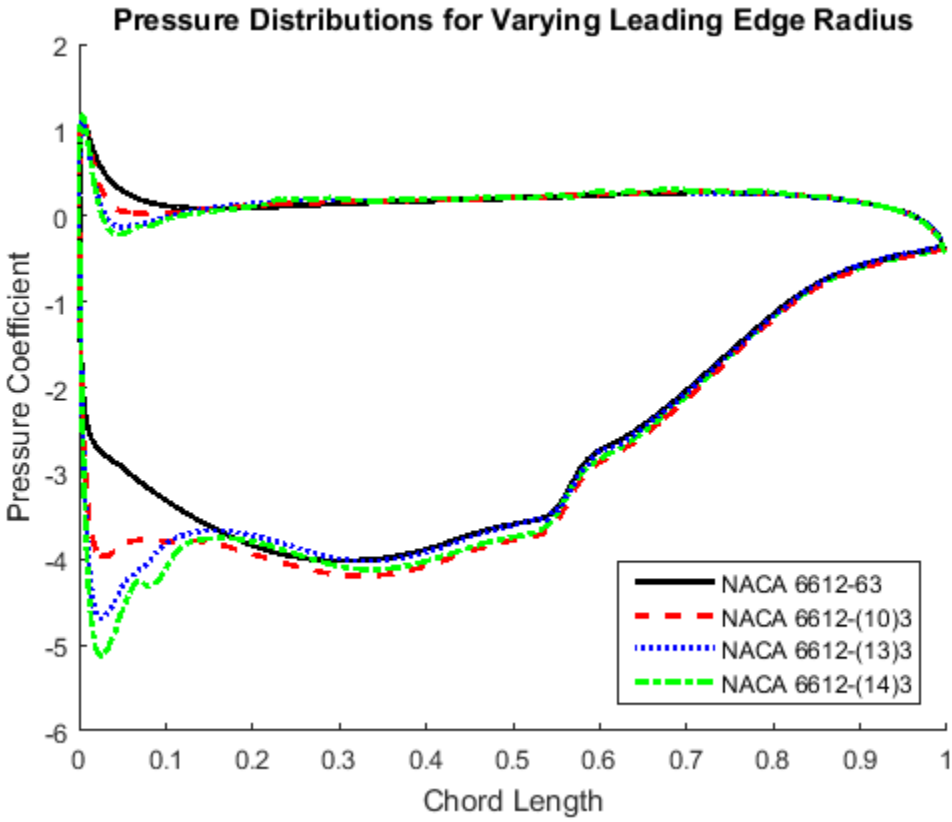


*Figure 24: pressure distributions for four airfoils with different leading edge radii*

While the suction increases with leading edge radius, there is a decrease in pressure on the pressure side, as well as a harsh transition to turbulent flow that results in the sudden decrease in downforce and increase in drag once increase leading edge radius beyond an index number of 13.

So, changing the leading edge radius is an effective way to increase the downforce of an airfoil. However, it is extremely sensitive when approaching the region of peak performance. Prior to that point, it does little in the way of changing downforce, drag, or lift to drag ratio until an initial peak is approached which leads to small increases in downforce with similar increases in drag. These result in stagnant efficiencies, but increasing the leading edge radius further begins to enhance all performance characteristics in a positive manner. Due to these effects and sensitivities, changing the leading edge radius may have adverse effects when coupled with other geometric parameters, or even general ride conditions. Changing lead edge radius seems highly useful to augment desired performance characteristics, but these further relations must be studied to ensure adverse sensitivities do not exist.

### 3.6: Trends for Varying Maximum Thickness Location

Previously, changing the maximum thickness of an inverted airfoil in ground effect, had all around positive results. When downforce increased, the drag decreased, and thus, the lift to drag ratio increased as well. Even when changing the location of maximum thickness, the general trends are very similar, and they are almost identical when looking at the downforce of Figure 25.

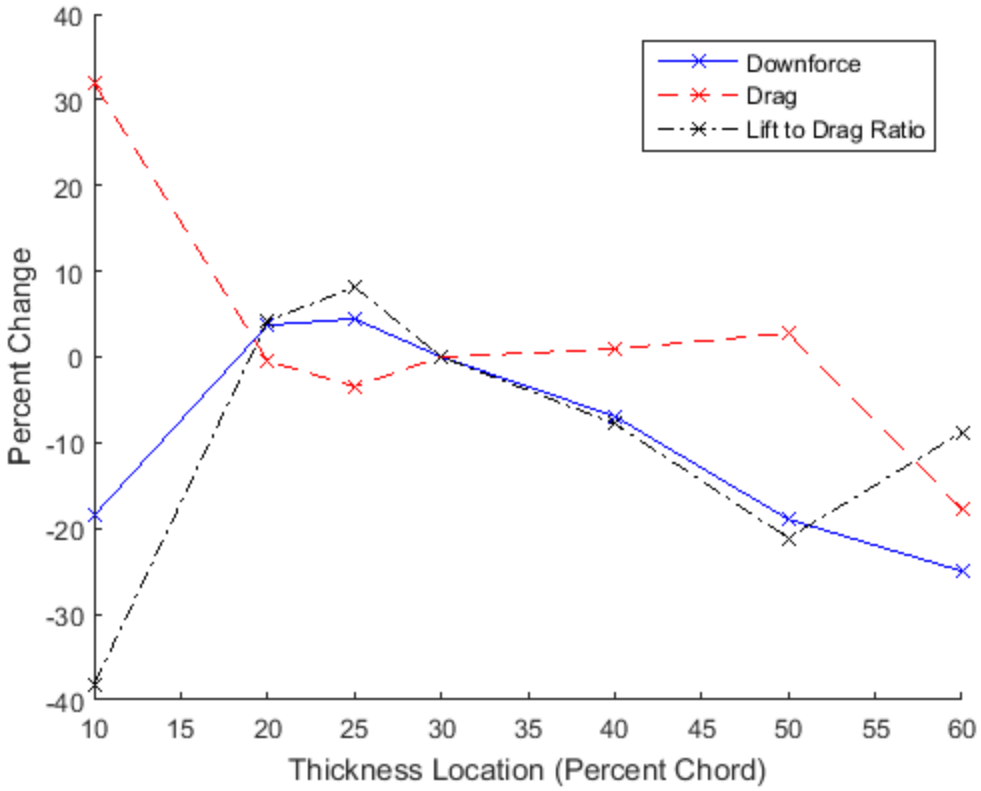


*Figure 25: trends in downforce, drag, and lift to drag ratio with respect to changing the location of maximum thickness*

The trend shows, just as in changing the maximum thickness, there is an initial spike as the distance from the leading edge is increased from 10% chord. Then, the peak is reached, and the downforce steadily decreases. However, the drag suddenly begins to drop and the lift to drag ratio spikes when the maximum thickness location gets to sixty percent chord. Unfortunately, the trends were limited due to the limitations of JAVAFoil for producing airfoil geometries. As the maximum thickness location moved beyond sixty percent chord, a lack of constraint on the trailing edge angle caused invalid airfoil geometries to be produced. In order to further study the maximum thickness location moving further aft, either a new software must be implemented to better handle these more extreme geometry changes, or a more constrained airfoil family must be tested.

Downforce production peaks when the location of maximum thickness is twenty-five percent chord. This location yields an increase in downforce of approximately 4.5% compared to the baseline NACA 6612-63. Comparing this to the previous results, this is a comparable change in downforce for any given local maxima. Just like changing the maximum camber location, the baseline configuration is very close to the local maxima. Similarly, having an appropriate location for the maximum thickness is important as significant decreases in downforce can occur otherwise. Having the maximum thickness location at ten or sixty percent chord results in a decrease in downforce of approximately 18.5 and 25% respectively. Again, while downforce can be moderately improved by adjusting the maximum thickness location, inappropriate positioning can result in large losses in performance. While all of these trends are similar to that of changing the maximum camber location, as they were seen to impact one another in Figure 18, they actually have a different relationship in this scenario illustrated by the pressure distributions of Figure 26.

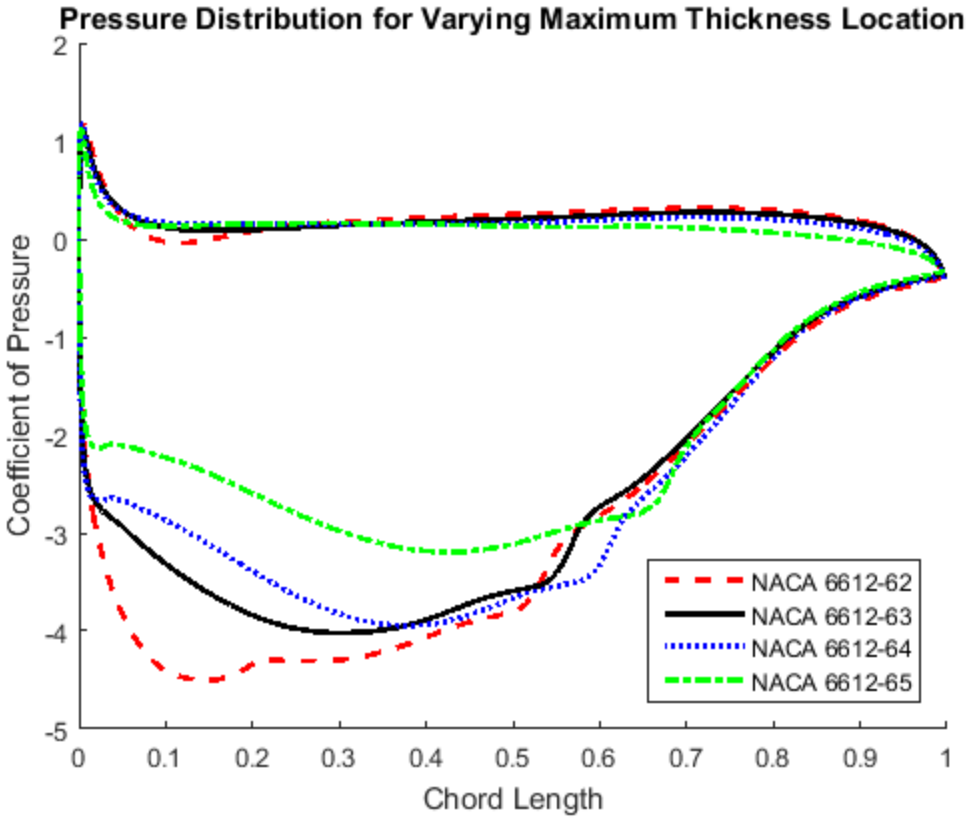


*Figure 26: pressure distributions for varying maximum thickness locations*

As seen in the figure, despite a majority of the geometry changing, the changes in the pressure distribution are concentrated in one particular region; the suction side forward of the maximum camber location. The suction peak developed still remains very near the location of maximum thickness. What is interesting to note is the interaction as it moves very far forward on the airfoil and begins to interact with the leading edge. The increased curvature near the front of the airfoil causes a spike in effective pressure on the suction side just as was observed in increasing the leading edge radius. Since the maximum thickness of the airfoil has moved forward as well, there is not a significant drop in the effective pressure as was seen with an increase in leading edge radius. However, this causes transition to occur earlier on the airfoil and decreases the effective pressure on the aft portion of the suction side of the airfoil. While moving the maximum thickness aft delays transition, improving the aft portion of the airfoil, it also

reduces the suction peak produced resulting in the losses in downforce observed in the previous section. Yet none of this shows a similar coupling that was seen when changing the maximum camber location. In changing the location of maximum camber the suction peak increased in magnitude as it moved toward the location of maximum thickness. But, in this instance, as the location of maximum thickness moves toward the location of maximum camber, the suction peak decreases. This shows that the coupling between these two parameters may not be as distinct as originally thought.

An observation of significance, is that large changes in drag occur near the extrema of the testing points, but there is little change in drag in between. Each of these extrema also yield opposite results. At ten percent chord, the location of maximum thickness yields an increase in drag of over 30%, while at sixty percent chord there is a decrease in drag of nearly 18%. It is important to note that the scope of this study excludes finding the location of maximum drag, and that the methods used for generating airfoil coordinates made it impractical to locate the location of minimum drag. However, there is a local minima in the data. This minima occurs when the location of maximum thickness is at roughly twenty-five percent chord. While small, there is a reduction in drag of approximately 3.4%. Despite this small change, it is important to remember that this is the location of maximum downforce production just as in changing the maximum thickness. This small change in drag is also not limited to the minimum drag configuration. With the maximum thickness located between twenty and fifty percent chord, there is never a change in drag of more than 3%. The reasoning for these changes in drag still have to do with the concentration in pressure on the upper surface of the airfoil, but Figure 27 shows that it is not acting in the same manner.

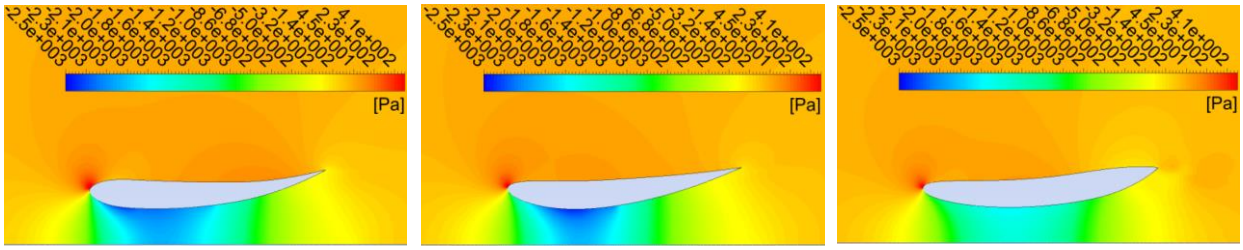


(a) (b) (c)

*Figure 27: pressure contours when adjusting maximum thickness location to 20% (a), 40% (b), and 60% (c) chord*

While the reduction of pressure and change in the resultant force vector are the causes for the decrease in drag when maximum thickness is sixty percent chord, it is not quite the same as previously seen. Due to the location of maximum thickness being at the same location as that of maximum camber, the pressure build up does not occur there any longer. Rather an acceleration of flow occurs from the increase in curvature mitigating this buildup of pressure drag. Although it does greatly reduce the suction peak on the lower surface, this reduction in pressure drag is far greater than the reduction of downforce resulting in a decrease in lift to drag ratio of less than nine percent when the location of maximum thickness is at sixty percent chord while it is a decrease of over 21% when at fifty percent chord.

Overall, changing the location of maximum thickness can result in increases in downforce through interactions with the leading edge suction. Despite seeing a significant relationship between the location of maximum camber and maximum thickness previously, changing the maximum thickness location seems to effect the suction peak in the opposite manner that occurred when the two came close together for changing the maximum camber location before resulting in a reduction in downforce in this instance. However, changing the location of maximum thickness has the largest impact when adjusting for reductions in drag. This is especially so if the maximum thickness is located further forward than twenty percent chord. Any further forward results in large losses of downforce, increases in drag, and thus, large

losses in lift to drag ratio as well. Whereas, moving the location further aft results in losses of downforce beyond twenty five percent chord, but there is a reduction in drag. This reduction becomes distinct beyond fifty percent chord, so much so that lift to drag ratio actually begins to increase again caused by the reduction of pressure drag concentration at the location of maximum camber on the upper surface. Unfortunately, the limitations of the airfoil production, or the family itself, resulted in inconclusive results for locations further aft than sixty percent chord. At the very least what can be taken away is that having the maximum thickness located around twenty five percent chord is useful for increasing downforce and lift to drag ratio, while having it located beyond fifty percent chord is useful for drag reduction.

# Chapter 4: Optimization

## 4.1: Problem Setup

As was stated in the previous sections, there is a great deal of complexity when considering potential interactions between the different geometric parameters. This renders the classical trend line studies that have been reported thus far insufficient for observing these higher order systems. One way in which to handle multivariable systems would be to utilize optimization techniques. For the studies done in the next several sections, the classical optimization technique of carpet plots was incorporated to determine the effects on the aerodynamic forces produced in a multivariable system. While still simple to create, carpet plots remove some of the complexities in viewing a multivariable system. This allows the inter-relations of the geometric parameters to be observed, and a minimum design point to be determined. However, this simplicity comes with a cost; the number of data points required to determine an optimum increases exponentially with the number of parameters. So, in order to effectively reduce the number of data points required, two variables were selected based on the preliminary constraints of the optimization as well as the cost function to be minimized.

First and foremost, a cost function had to be determined. Due to the nature of implementing aerodynamics in race cars from a design perspective, it is difficult to focus on any single parameter to get a robust view of design implications. For this reason there will be three minimizations for three different cost functions. In order to have a quality design comparison, all of the constraints will be held constant throughout. As has been emphasized in the previous discussions, the three potential cost functions to minimize would be lift, drag, and lift to drag ratio. Again, emphasis will be put on the fact that negative lift is desired, so minimizing lift and

lift to drag ratio can also be looked at as maximizing downforce and the corresponding lift to drag ratio.

For this set of optimizations, the baseline NACA 6612-63 airfoil will be used again as a baseline. In order to obtain an optimum, constraints need to be placed upon the system to ensure the solution will not be unbounded. Due to the negative impact that drag has upon the performance of race cars and the importance of maintaining a high lift to drag ratio, these two performance characteristics will be used as constraints. Since the primary reason for implementing wings on a race car is the production of downforce, the downforce will be used as a constraint as well. For these three performance constraints, each one will be held constant. In other words for each optimization the resulting optimum will produce at least as much downforce as the NACA 6612-63, and have drag less than or equal to this baseline. They will also have a lift to drag ratio greater than or equal to the 6612-63. Because of these limitations, the geometric parameters that could be implemented in optimization were then reduced.

Looking back at the figures in section 3.1, it can be seen that nearly every trend is dominated by the changes in maximum camber. Therefore, to get the most significant changes, maximum camber was selected as one of the variables for optimization. The trends show though, that adjusting the maximum camber to gain more downforce resulted in large increases in drag. So, in order to utilize the benefits of adjusting the maximum camber, the other geometric parameter must decrease drag while also increasing downforce. It is this issue that immediately eliminates the maximum camber location as a suitable partner to be used in optimization. That leaves three options; maximum thickness, leading edge radius, and the maximum thickness location. Since it consistently yielded the second most gains in downforce in the previous testing,

as well as showing only positive changes in performance all around, maximum thickness was selected as the second variable for optimization.

Before optimization even begins, more constraints still need to be defined. Even though there are three performance constraints, constraints still need to be placed on the geometry of the airfoil. Primarily, this is in order to have a wing that can handle the variations in conditions that occur on track to avoid stall. Looking back to the previous sections it can be seen that reducing the thickness of the airfoil beyond six percent chord, or increasing camber beyond nine percent chord resulted performance reductions from stall. This then gives the increment of displacement from the baseline to create the test matrix. So, for this optimization, a 3x3 matrix was used to form the carpet plot. The maximum camber was tested at three, six, and nine percent chord while the thickness was tested at six, twelve, and eighteen percent chord. This was set up with the desired outcome to be several designs that would meet the performance criteria and several that would not. With this design matrix, a carpet plot was formed with performance constraints being that the optimum could not produce less downforce, more drag, or have a worse lift to drag ratio than the NACA 6612-63 as well as geometric constraints to avoid stall limiting camber to at most nine percent chord and thickness to no thinner than six percent chord.

### 4.2.1: Minimizing Lift (Maximizing Downforce)

In looking at the carpet plot in Figure 28 the active constraints for minimizing the lift of an inverted airfoil in ground effect are the drag and thickness constraints.

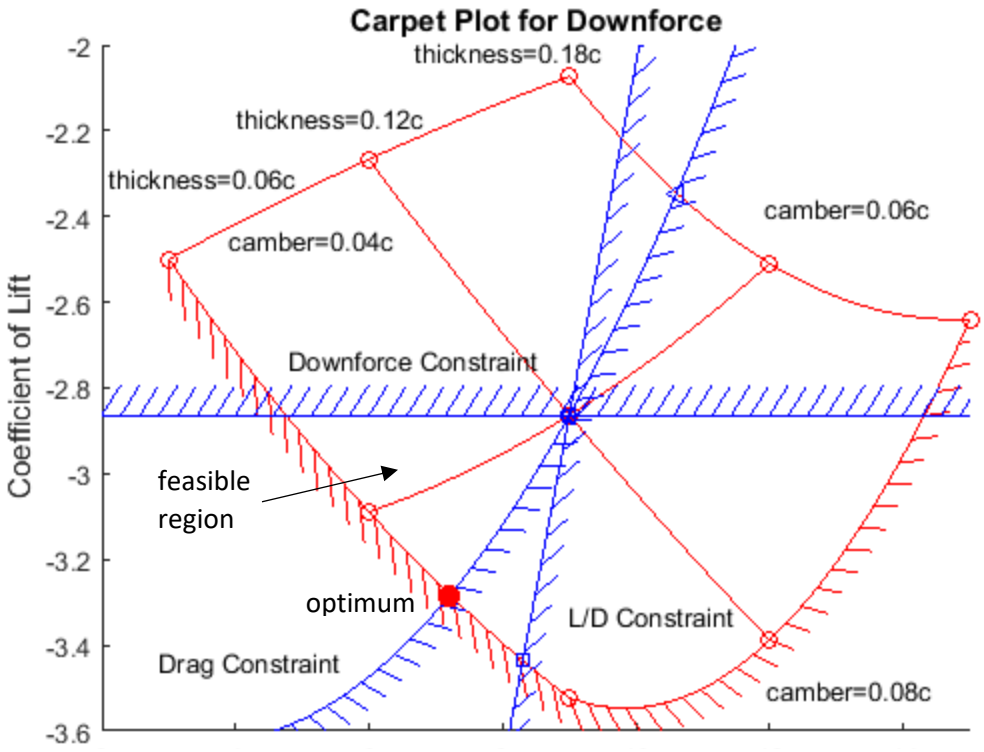


*Figure 28: carpet plot for minimizing lift*

The resulting optimum in the model had a maximum thickness of six percent chord and a maximum camber of just over seven percent chord. While it did not impact the overall results obtained by the carpet plot, it is important to note that Fluent was not able to sufficiently handle the lowest thickness and cambered airfoil tested. Therefore, an artificial value that better fit the trends was inserted in its place. This change is discussed in the next section and did not affect the optimum. Overall, the optimum geometry resulted in an increase in downforce of 15%. This increase in downforce is nearly the largest gain seen from any single parameter change. Again, this is without any increase in drag or loss in the lift to drag ratio, whereas to get this increase with camber alone resulted in an increase in drag of 47% and a decrease in lift to drag ratio of 22.7%. If the drag constraint were allowed to vary by ten percent, the changes in downforce

would be less than 3%. So, it appears that unless drag is changed significantly, the overall downforce may not change much.

However, since the drag did not increase while the downforce did, the lift to drag ratio actually increased by nearly 15%. This change in lift to drag ratio is nearly identical to that of reducing the maximum camber to under five percent chord, which resulted in a loss of downforce of over 6%. The equivalent change in maximum thickness alone would be reducing it to less than six percent chord which results in a gain in downforce of only 2.5%.

This shows just how highly coupled the entire system is because, while both can achieve similar gains in the lift to drag ratio, neither of them can do so with the enormous gains in downforce that the optimum experiences. As stated before, while camber can increase downforce a similar amount, it cannot do so without significant penalties that can be avoided with the optimization process. Yet still, there could potentially be even more gains for the entire system if a higher order optimization technique were to be utilized. This is especially so considering the advantages that the leading edge radius and maximum thickness location had similar effects to that of the maximum thickness. Overall, more research would be required to figure out just how much more performance can be obtained.

### 4.2.2: Minimizing Lift Analysis

To add validity to the model developed with the carpet plot, the optimum airfoil was tested in Fluent. The carpet plot proved to be highly accurate, as the largest error found in any given aerodynamic value was just over 1% of the predicted value. So, the data discussed previously is highly valid for interpolation of the computational results developed throughout the process. But, this still begs the question as to why the optimum is so effective as well as what

happens when the geometric parameters are coupled.

Looking at the pressure distributions of Figure 29, there are a great deal of shared qualities between the optimum pressure distribution and the individual changes to the geometric parameters.

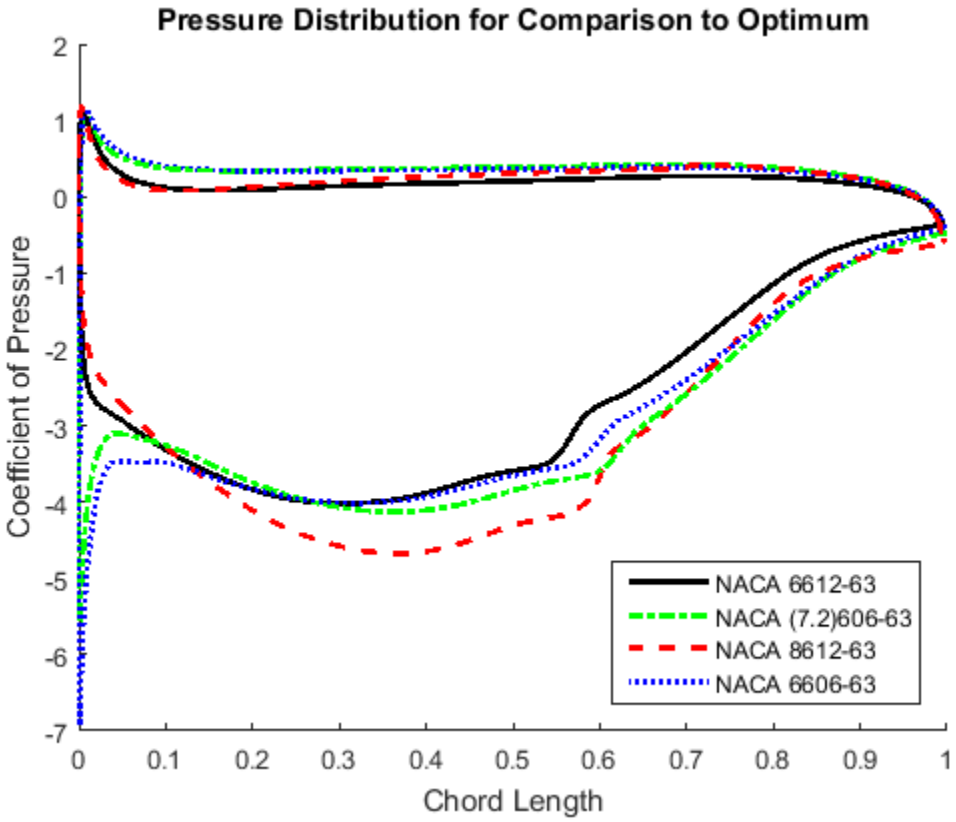


*Figure 29: the pressure distributions comparing the baseline, optimum, and two similar, isolated geometric parameter changes tested previously*

As has been the case throughout this entire study, the changes to the suction side dominate the production of downforce. The adjustment to the thickness causes a reduction to the leading edge radius, which develops a defined split to the flow, causing an increase in the effective pressure around the leading edge of the airfoil. There is also an increase in the effective pressure throughout the entire pressure side as well. Also, the transition to turbulence is delayed, again increasing the effective pressure near the trailing edge. What is interesting is that these features

from the change in thickness dominate the trends for the pressure distribution of the optimum despite changes in camber dominating the general trends in Chapter 3.

Therefore, when comparing the maximum thickness and the maximum camber, the maximum thickness is actually the dominating geometric parameter for the pressure distributions. Thus, changing the maximum camber can be utilized to augment the performance of the airfoil with respect to changing the maximum thickness. Just as before, when increasing the maximum camber the suction peak began to increase and move toward the location of maximum camber. However, due to the dominant nature of the maximum thickness in the trends, as well as the increased suction at the leading edge, this resulted in the effective area of the suction peak increasing with only a minor decrease in the effective pressure. This becomes distinct through observing the velocity contours of Figure 30.

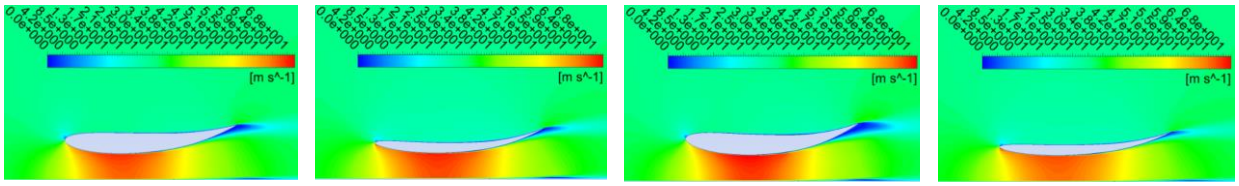


(a) (b) (c) (d)

*Figure 30: velocity contours for the NACA 6612-63 (a), optimum (b), 8612-63 (c), and 6606-63 (d)*

While increasing the maximum camber increased the magnitude of the high velocity region, the effective area it covered was greatly reduced. Meanwhile changing the maximum thickness led to an increase in the high velocity around the leading edge of the airfoil on the suction side. In coupling these two geometric characteristics, the high velocity region not only increased in magnitude due to the change in camber, but the bias toward the maximum camber location as well as the increased velocity near the leading edge caused a much greater effective area to develop. This explains the increase in downforce that developed, although the change in

thickness did cause the region of flow separation to decrease. This would result in a decrease in drag, but as the results have shown, it should be the same as the NACA 6612-63. The pressure contours of Figure 31 highlight the reasoning as to why.

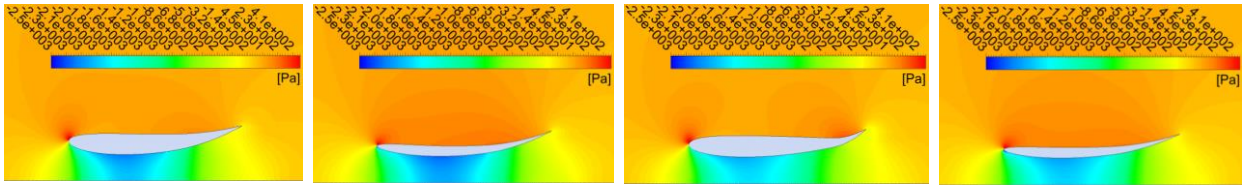


(a) (b) (c) (d)

*Figure 31: pressure contours for the NACA 6612-63 (a), optimum (b), 8612-63 (c), and 6606-63 (d)*

Looking closely at the pressure side, while there is an increase in the effective pressure as there was with decreasing the maximum thickness of the airfoil, the change in camber comes back into play. This increase to the curvature of the pressure side adds a bias in the effective pressure toward the location of maximum camber. In doing so, the effective pressure is higher on the pressure side while still having a similar distribution as seen on the baseline. Like in increasing the maximum camber, this will result in an increase to the drag contribution of the airfoil. It is this contribution that offsets the reduction in drag that is experienced through the reduction of flow separation.

So, the maximum thickness dominates the characteristics of the pressure distributions making it the primary variable when trying to produce downforce. Increasing the maximum camber adjusts the pressure distribution to augment the downforce produced, and combined with the increased suction at the leading edge, increase the area of effective pressure for the suction peak. However, when drag is the primary concern, camber clearly dominates the trend due to its effects on the pressure side of the airfoil. By increasing the curvature on the pressure side, more drag is developed which offsets the reduction in flow separation that comes with reducing the

thickness of the airfoil for the optimum. All of this allows for the large gains in downforce listed earlier without any negative effects on the drag or lift to drag ratio.

### 4.2.3: Other Design Considerations

While finding the optimum to maximize downforce is an important consideration for design, it must not be forgotten that an inverted airfoil in extreme ground effect is utilized primarily for the development of the front wing of race cars. So, it is vital to always remember that in order to maximize performance, the wake behind the wing will have considerable effect on any aerodynamic devices implemented behind the wing. Therefore, reducing the impact of the wake may outweigh gains in downforce if there is a detrimental impact on the flow behind the wing which would ruin the performance of other aerodynamic devices.

Looking at the wakes of Figure 32 it can be seen that the optimum airfoil and the NACA 6606-63 share a very similar wake.

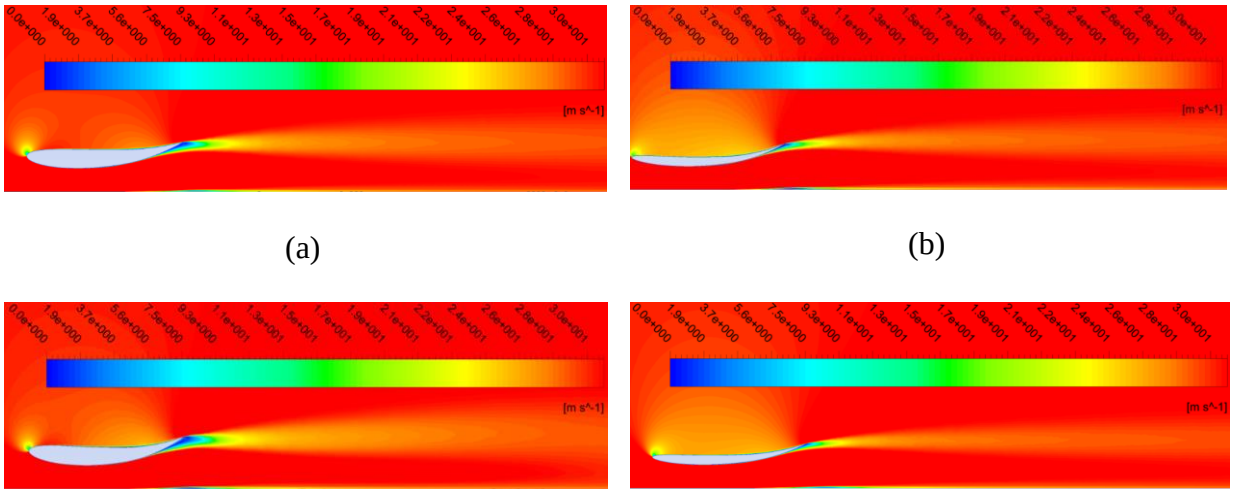

(a) (b)

(c) (d)

*Figure 32: wakes behind the NACA 6612-63 (a), optimum (b), 8612-63 (c), and 6606-63 (d)*

Both have a smaller wake compared to the baseline NACA 6612-63 airfoil. Looking at the far field behind the airfoils it can be seen that the wake dissipates quickly, although the flow still does not recover to freestream velocity. However, in the near field, it can be seen that the optimum has a larger wake near the trailing edge. This increase in the near field disturbance is caused by the increase in camber that allows for the increase in downforce for the optimum. It is the change in camber that has the largest impact on the wake behind the airfoil. Not only does the NACA 8612-63 have a larger wake than any of the other airfoils displayed due to the increased amount of flow separation, it also has a larger disturbance to the far field which dissipates much further downstream.

So, optimizing the airfoil to maximize downforce had a positive effect on the wake following the airfoil. However, this was only because the decrease in thickness which resulted in a lower region of flow separation at the trailing edge. Had the airfoil become thicker, or the camber increased, the wake would have become larger than that of the baseline configuration. If it were desired to reduce the wake, a decrease in the camber could be implemented to further reduce the flow separation acting upon the airfoil.

### 4.3: Minimizing Drag/Lift to Drag Ratio

When minimizing the drag seen in Figure 33, the active constraints again include the maximum thickness being six percent chord or higher and maintaining the same downforce as the baseline.

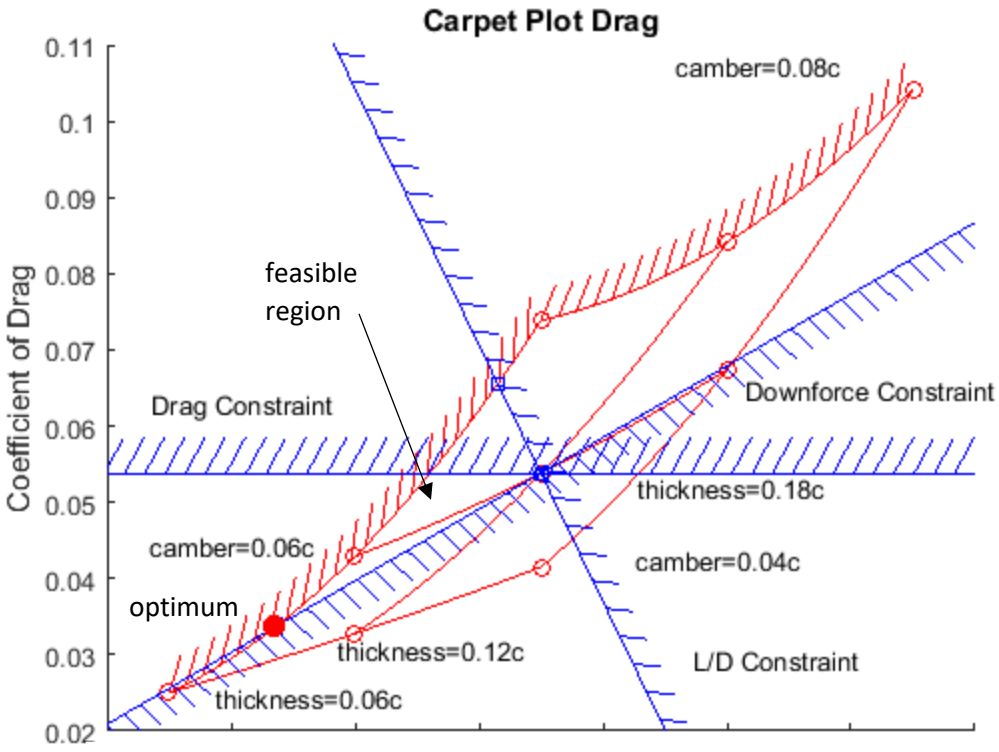


*Figure 33: carpet plot for minimizing drag*

As a result of the high impact that the drag has on the lift to drag ratio, maximizing the lift to drag ratio yields the same optimum point. So, this model resulted in an airfoil that was six percent chord thick and had a maximum camber of four point seven percent chord. This model predicts that this would result in a reduction of drag of over 37% which corresponds to a lift to drag ratio that would be nearly 60% higher. If only camber were adjusted it would need to be reduced to under four percent chord to reduced drag as much, but this would reduce the downforce produced by over 12.5%. Even with this ability to reduced drag, a similar increase in lift to drag ratio with camber alone is not achievable. Interestingly enough, despite the gains achieved in lift to drag ratio utilizing the maximum thickness since it increased downforce and decreased drag at its most effective points, it still could not match the lift to drag ratio increase or drag decrease of the optimum. So, due to either the performance limitations of the geometric

parameters, or their pro and con nature in performance, neither could achieve a similar lift to drag ratio. Even changing the maximum camber, which dominated all of the trends, was only sufficient in decreasing the drag with a severe cost in the downforce produced.

### 4.3.2: Minimizing Drag/Lift to Drag Ratio Analysis

Unfortunately, due to the thinness and low camber of the airfoil, the Fluent setup was plagued by the same problems that required estimation of the NACA 3606-63 airfoil data. This means that the estimation that had no effect on the optimization and prediction of downforce is a majority of the input for the predicted values in the previous section. Therefore, a more robust method will need to be developed to handle the changes in geometry more effectively in order to verify that the carpet plot results are plausible.

# Chapter 5: Conclusion and Future Studies

## Chapter 5.1: Conclusion

The focus of this investigation was to analyze the geometric parameters that define the modified NACA 4 Series airfoil family in ground effect, analyze the aerodynamic characteristics of each of these parameters, and determine two key parameters to be used for an optimization utilizing carpet plots. In performing individual parametric studies, it was found that changing the maximum camber of the airfoil caused the greatest increases in downforce, but also came with a heavy drag penalty. Given that one of the constraints for this optimization process was to have no more drag than the baseline NACA 6612-63 airfoil, the other parameter selected for the optimization process would have to be capable of reducing drag. However, since the goal was to maximize downforce (minimize lift), the coupled parameter would ideally increase downforce as well as reduce drag. These characteristics were found for changing the maximum thickness, maximum thickness location, and leading edge radius; although changing maximum thickness had a greater total change in both downforce and drag so it was selected for optimization.

Through the individual parametric studies, one of the constraints placed on the problem was that of stall due to decreased thickness. This became one of the two active constraints that defined the optimum point, the other being that of maintaining constant drag. While not active, two other constraints had been placed upon the problem; stall due to increased camber, and having at least the same lift to drag ratio. The optimum when varying the maximum camber and thickness resulted in a maximum camber of 7.2% chord and a maximum thickness of 6% chord. Analyzing this airfoil configuration revealed an increase in downforce of over 15%. It was this process of coupling the geometric parameters that revealed that downforce was most closely related to the maximum thickness of the airfoil despite the largest changes in the parametric

studies coming from varying the maximum camber. Camber was still dominant in the production of drag, as would be expected, resulting from the large increases in pressure drag due to the increased curvature of the upper side of the airfoil.

Future work would include a refined computational model to work directly with optimization results. Other work to assist with this would be to develop a robust set of wind tunnel data to validate that the model can handle potentially extreme changes in geometry that could be occurring. Other studies would also be a more in depth analysis using carpet plots for higher order systems, or using an entirely different optimization technique to mitigate the drawbacks of carpet plots. Comparisons could also be performed in relation to the automated systems of optimization that are built in to ANSYS Fluent to determine the robustness of such tools.

## References


[1] Sylt, Christian. "F1 Teams Race Off With $1.5 Billion Revenue." *Forbes*. Forbes Magazine. (2016).

[2] Dominy, R. G. "Aerodynamics of grand prix cars." *Proceedings of the Institution of Mechanical Engineers, Part D: Journal of Automobile Engineering* 206.4 (1992). pp. 267-274.

[3] Zhang, Xin, Willem Toet, and Jonathan Zerihan. "Ground Effect Aerodynamics of Race Cars." *Applied Mechanics Reviews* 59.1 (2006). pp. 33-49.

[4] Ahmed, Mohammed R., and S. D. Sharma. "An investigation on the aerodynamics of a symmetrical airfoil in ground effect." *Experimental Thermal and Fluid Science* 29.6 (2005). pp. 633-647.

[5] Ahmed, M., T. Takasaki, and Y. Kohama. "Experiments on the Aerodynamics of a Cambered Airfoil in Ground Effect." *44th AIAA Aerospace Sciences Meeting and Exhibit*. 2006.

[6] Ahmed, Mohammed R., T. Takasaki, and Y_ Kohama. "Aerodynamics of a NACA4412 Airfoil in Ground Effect." *AIAA Journal* 45.1 (2007). pp. 37-47.

[7] Ranzenbach, Robert, and Jewel B. Barlow. “Two-dimensional Airfoil in Ground Effect, an Experimental and Computational Study.” No. 94-2509. SAE Technical Paper, 1994.

[8] Ranzenbach, Robert, and Jewel Barlow. "Cambered Airfoil in Ground Effect: Wind Tunnel and Road Conditions." *13th Applied Aerodynamics Conference*. 1995.

[9] Ranzenbach, Robert, and Jewel Barlow. “Cambered Airfoil in Ground Effect: an Experimental and Computational Study.” No. 96-0909. SAE Technical Paper, 1996.

[10] Zerihan, Jonathan, and Xin Zhang. "Aerodynamics of a Single Element Wing in Ground Effect." *Journal of Aircraft* 37.6 (2000). pp. 1058-1064.

[11] Abbott, Ira Herbert, and Albert Edward Von Doenhoff. *Theory of Wing Sections, Including a Summary of Airfoil Data*. Courier Corporation, New York, 1959.

[12] Katz, Joseph. *Race Car Aerodynamics: Designing for Speed*. R. Bentley, Cambridge, MA, 2006.

[13] McBeath, Simon. *Competition Car Aerodynamics: A Practical Handbook*. Haynes, Sparkford, UK, 2011.

[14] Zerihan, Jonathan, and Xin Zhang. "Aerodynamics of Gurney flaps on a Wing in Ground Effect." *AIAA Journal* 39.5 (2001). pp. 772-780.

[15] Zhang, Xin, and Jonathan Zerihan. "Aerodynamics of a Double-Element Wing in Ground Effect." *AIAA Journal* 41.6 (2003). pp. 1007-1016.

[16] Qin, Xuguo, Peiqing Liu, and Qiulin Qu. "Aerodynamics of a Multi-Element Airfoil near Ground." *Tsinghua Science & Technology* 14 (2009). pp. 94-99.

[17] ANSYS, Inc. *ANSYS Fluent User's Guide*. Canonsburg, PA: ANSYS, Inc. (Release 15, November 2013).

[18] Ladson, Charles L., et al. "Computer program To Obtain Ordinates for NACA Airfoils." NASA Technical Memorandum 4741. (1996).

[19] Mahon, Stephen, and Xin Zhang. "Computational Analysis of Pressure and Wake Characteristics of an Aerofoil in Ground Effect." *Journal of Fluids Engineering* 127.2 (2005). pp. 290-298.

[20] ANSYS, Inc. *ANSYS Fluent Theory Guide*. Canonsburg, PA: ANSYS, Inc. (Release 15, November 2013).

[21] Genua, Emanuela. “A CFD Investigation of an Inverted Airfoil in Ground Effect.” Delft University of Technology. (2009).

[22] Raymer, Daniel P. *Aircraft Design: A Conceptual Approach*. Reston, VA: American Institute of Aeronautics and Astronautics. (2012).

# Appendix A

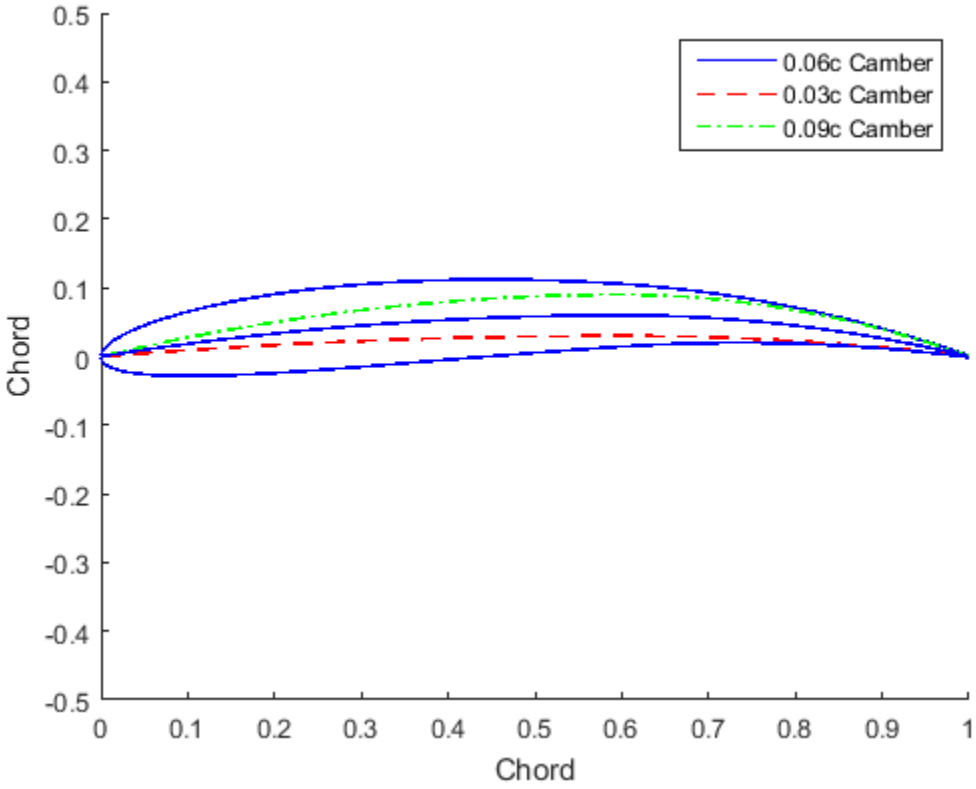


*Figure 34: representation of varying maximum camber*

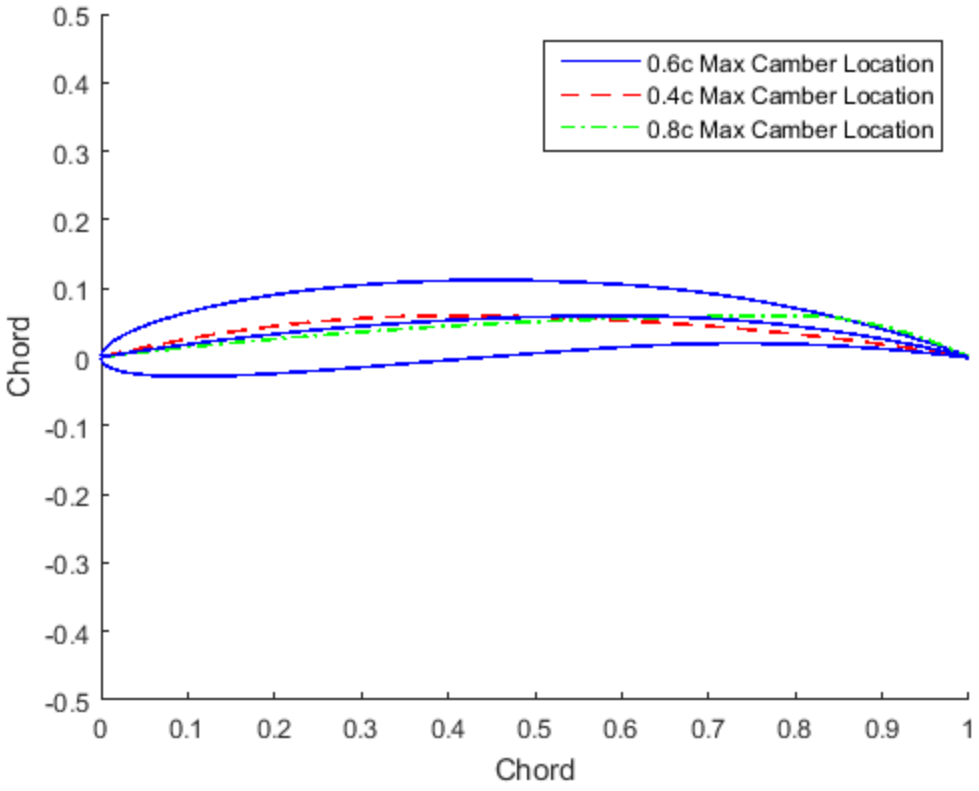


*Figure 35: representation of varying maximum camber location*

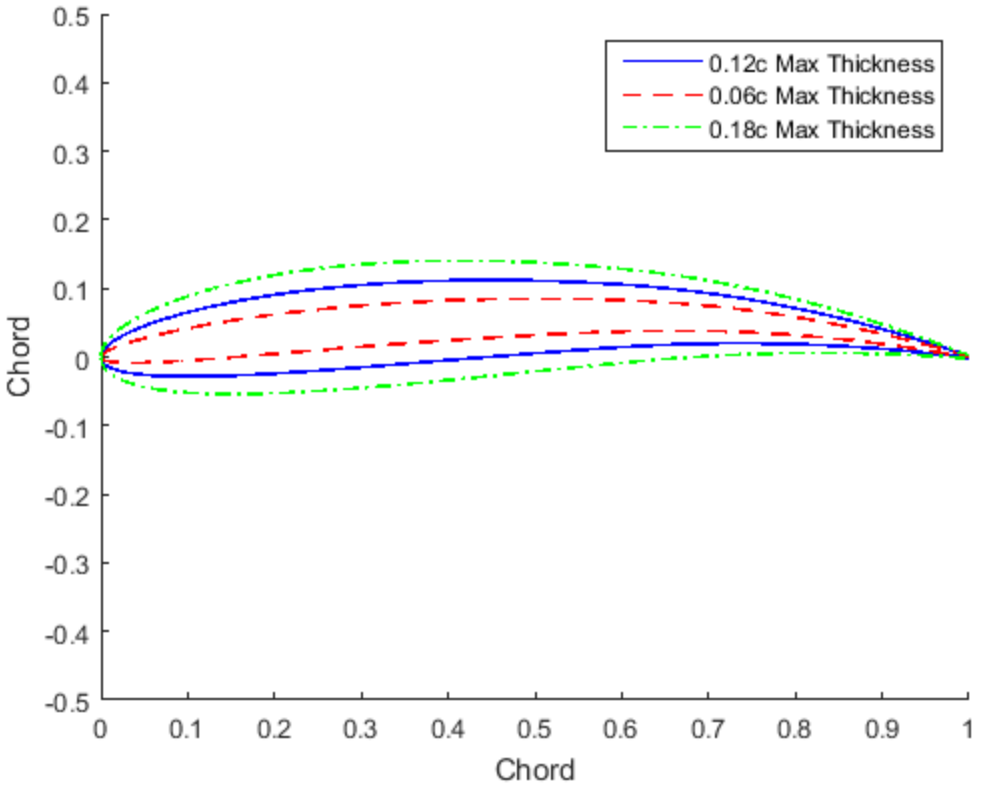


*Figure 36: representation of varying maximum thickness*

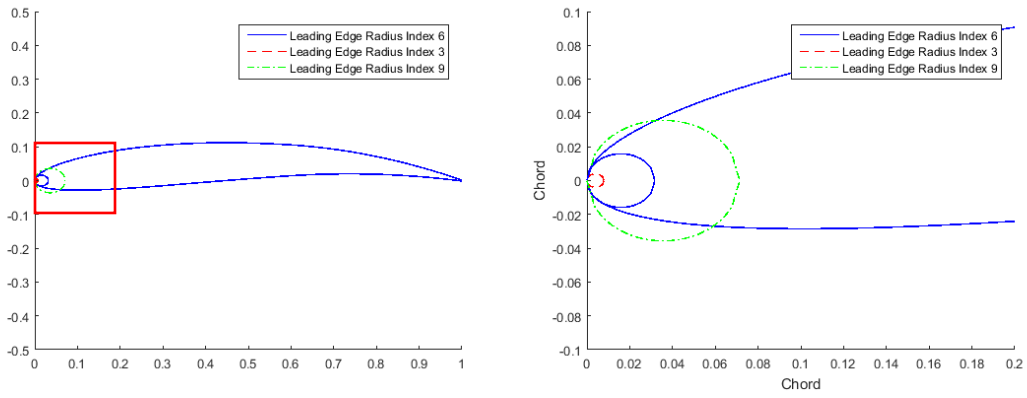


*Figure 37: representation of varying leading edge radius*

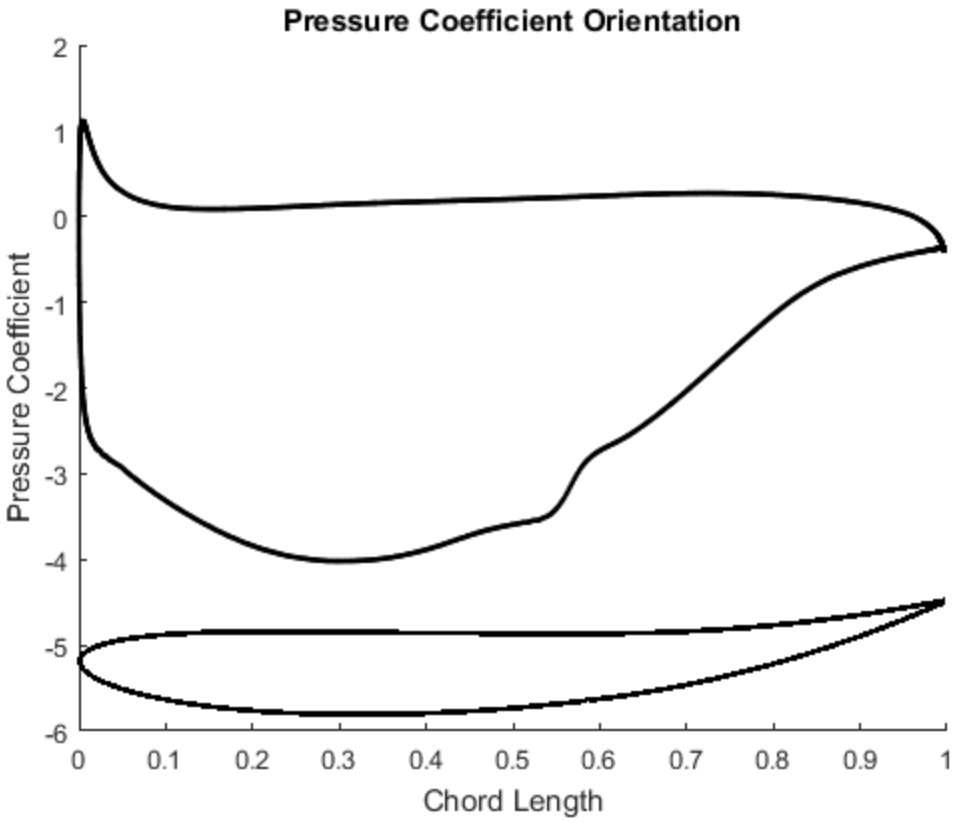


*Figure 38: orientation of pressure distribution with baseline NACA 6612-63 airfoil*

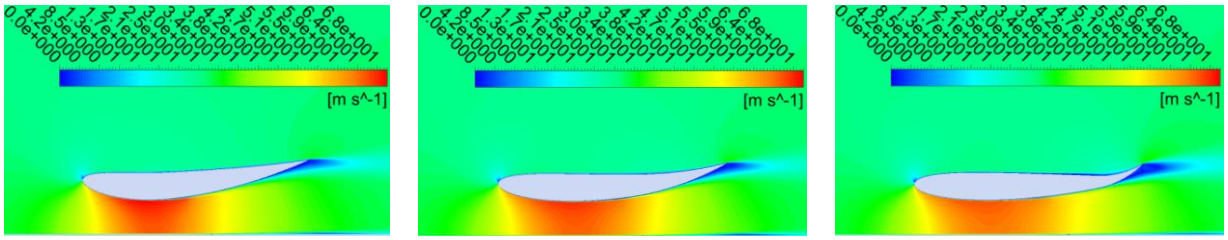


(a) (b) (c)

*Figure 39: velocity contours when changing the maximum camber location from 40% (a), 60% (b), and 80% (c)*

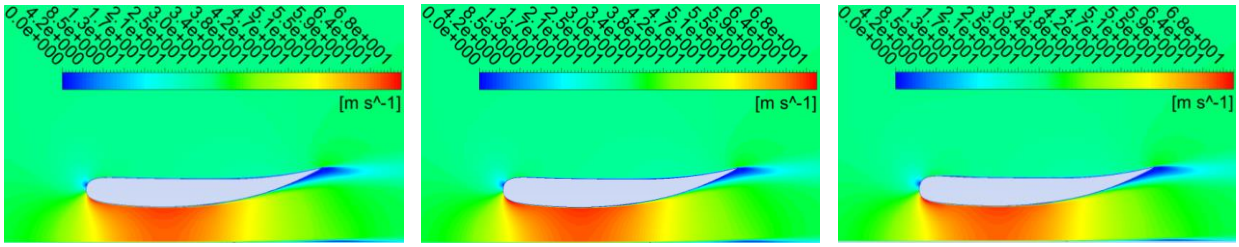


(a) (b) (c)

*Figure 40: velocity contours for increasing leading edge radius with corresponding index numbers 12 (a), 13 (b), and 14 (c)*

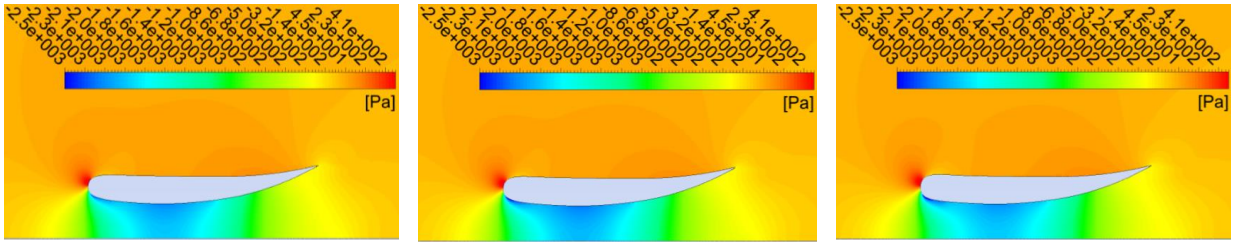


*Figure 41: pressure contours for the previous velocity profiles*

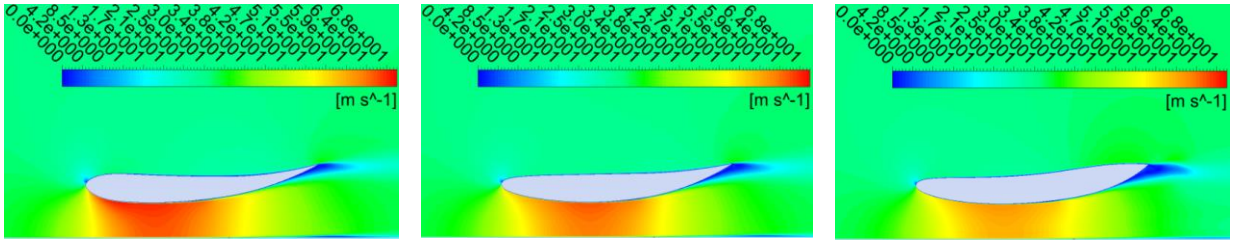


(a) (b) (c)

*Figure 42: velocity contours when adjusting maximum thickness location to 20% (a), 40% (b), and 60% (c) chord*